On the Passive Force Closure Set of Planar Grasps and Fixtures

Amir Shapiro* Dept. of ME, Ben Gurion University, ashapiro@bgu.ac.il

Elon Rimon Dept. of ME, Technion, rimon@technion.ac.il

Shraga Shoval Dept. of IE, Ariel College, shraga@ariel.ac.il

Revised on January 2010

Abstract *This paper considers grasps and fixtures whose contacts react according to force-displacement laws consistent with friction constrains at the contacts. The* passive force closure set *of such grasps and fixtures is the set of external wrenches (forces and torques) that can act on the grasped object and be stably balanced by the contacts. An external wrench belongs to this set if it induces a feasible equilibrium whose basin of attraction contains the initial unperturbed grasp configuration. The paper focuses on planar grasps and fixtures having sharp-tipped fingers or fixels that satisfy linear force displacement laws. Using Morse Theory, the paper characterizes the number and stability type of k-contact equilibria induced by a given external wrench. Based on this analysis, the paper provides closed-form expressions for the passive force closure set of k-contact grasps and fixtures. Computation of the allowed external wrenches is illustrated with examples. Finally, the paper describes experiments verifying the passive force closure set on a spring-loaded grasping system.*

1 Introduction

This paper considers grasps and fixtures of a rigid object by frictional fingertips or fixels in a planar environment. The classical notion of *force closure* requires that the contacts be able to actively balance any disturbance wrench (force and torque) acting on the grasped object [2, 28]. Force closure is a generic property of frictional equilibrium grasps [20, 38], and it ensures that the grasp is locally controllable [3, 20]. However, the notion of force closure does not specify *how* the contacts should balance a given disturbance wrench. Moreover, once specific reaction laws are deployed in a given grasping or fixturing system, only a bounded set of external wrenches can be balanced by the contacts. In order to synthesize safe manipulation plans for the grasped object, one needs tools for computing the set of external wrenches that can be stably balanced by the contacts [16, 29]. An analogous situation arises when a limbed robot braces itself against tunnel walls during quasistatic locomotion [26]. In order to synthesize safe locomotion plans, the robot needs to determine which disturbance wrenches generated by its moving limbs can be stably balanced by the contacts.

*Corresponding author: Dept. of ME, Ben Gurion University, Israel.

When the fingertips or fixels react according to pre-specified force displacement laws, the collection of external wrenches that can be stably balanced by the contacts is defined as the *passive force closure set.* This paper strives to characterize the passive force closure set of the following grasps and fixtures. First, the paper considers planar grasps and fixtures that may be influenced by a two-dimensional gravitational field. While the notion of passive force closure applies to planar as well as spatial grasps, its global analysis is significantly simpler in the case of planar grasps. Second, the paper focuses on the interaction of rigid fingertips or fixels with a perfectly rigid object. This is a reasonable assumption for fingertips and fixels made of metallic or hard-plastic materials, and for bulky objects that do not contain slender sub-structures. Third, the paper attempts to perform global stability analysis, therefore it assumes that the contacts react with linear force displacement laws. The implementation of such laws is discussed below. The paper further limits its scope to sharp-tipped fingers or fixels. This assumption provides a good approximation for fingertips or fixels whose curvature is significantly higher then the grasped object curvature [30]. Moreover, sharp-tipped fingers allow implementation of finger reaction laws using the fingers' internal joint sensors, without any need for sophisticated contact force sensors [22]. The paper's objective is thus to characterize the passive force closure set of k-contact grasps and fixtures governed by linear force displacement laws.

The related literature. The local stability of grasps and fixtures is generally determined by their *stiffness matrix*, giving the linearized relation between small movements of the grasped object and the net reaction wrench generated by the contacts. When the contacts are governed by reactive force-displacement laws, the stiffness matrix represents the Hessian of the grasping system potential energy i.e., the elastic energy stored at the contacts and the gravitational potential energy. Hanafusa and Asada [10] were the first to investigate the stiffness matrix of spring loaded grasping systems. Working in the context of frictional contacts and sharp-tipped fingers, Erdmann [7, 8] showed how to represent the friction cone constraint in the grasped object configuration space. Nguyen [20] characterized the stiffness matrix of general grasp arrangements obeying linear force-displacement laws. Nguyen also posed the problem of synthesizing linear force-displacement contact laws that would give a desired grasp stiffness matrix. This problem was subsequently investigated by Shimoga and Goldenberg [33], and has been fully solved by Huang and Schimmels [12, 13]. The stiffness matrix analysis and synthesis has been extended to curved fingers by Montana [19], Ponce [23], and Xiong et al. [35, 36]. A stable stiffness matrix ensures stability of the grasped object with respect to local position and velocity perturbations. We shall see that a stable stiffness matrix also ensures grasp stability with respect to a local neighborhood of disturbance wrenches. However, there has been no attempt in the literature to characterize this wrench neighborhood for a given grasp or fixture arrangement. This paper characterizes this wrench neighborhood in the simplest setting of linear force-displacement contact laws.

A common approach in the grasping literature is to lump the complex kinematic structure of the grasping mechanism into force-displacement laws at the contacts. However, when the kinematic structure of the grasping mechanism is taken into account, not all contact forces are necessarily realizable [5]. Consequently local grasp stability must be analyzed with respect to the entire mechanism [1, 38]. While these considerations are important in applications such as whole arm grasps [11, 21], here we simply assume that each finger is capable of generating its own linear force-displacement law. The implementation of such fingertip laws requires nonlinear cancellation of the finger's inertial forces. A control scheme for

achieving this behavior is described in an appendix of this paper. Linear force-displacement laws can also be directly implemented with spring-loaded devices similar to the ones deployed in our experiments (see Figure 9). The results of this paper are therefore useful not only for grasping applications, but also for light-duty fixturing tasks such as part assembly and material delivery [4, 27, 34].

The paper's structure and contributions are as follows. Section 2 introduces the notion of passive force closure suitable for grasps and fixtures governed by reactive force displacement laws. Section 3 describes the passive force closure set of grasps and fixtures governed by linear force displacement laws. This section contains two key results. First, no matter how many contacts participate in the grasp, every external wrench can be passively balanced at one or two stable equilibria of the grasped object. Moreover, the stable equilibria can be computed in closed form as a function of the external wrench. Second, the basin of attraction of the stable equilibria can be globally characterized using Morse Theory. These results provide expressions that determine if a given external wrench induces a feasible equilibrium whose basin of attraction contains the object's initial unperturbed equilibrium, thus determining if the external wrench belongs to the passive force closure set. Section 3 contains examples illustrating how specific external wrenches relate to the passive force closure set. Section 4 discusses the transient trajectory of the grasped object under the influence of an external wrench. Section 5 verifies certain aspects of the passive force closure set on a spring-loaded grasping system. The concluding section discusses open problems associated with computation of the passive force closure set in more general settings. Several appendices provide proof details; the last appendix describes a control scheme for achieving linear force-displacement laws at the grasping fingertips.

2 Review of Force Closure Grasps

This section reviews the notion of force closure and its local stability properties. Then it introduces the linear contact laws and the notion of passive force closure associated with such laws.

2.1 Frictional Grasp Terminology

We consider planar grasps and fixtures in which a rigid object $\mathcal{B}$ is held via frictional point contacts by rigid bodies $\mathcal{A}_1 \ldots \mathcal{A}_k$ representing fingertips or fixels. The analysis of $\mathcal{B}$'s motions takes place in its configuration space, or *c-space*, which is parametrized as follows (Figure 1). Let $d \in I\!R^2$ and $R(\theta) \in I\!R^{2\times 2}$ denote the position and orientation of $\mathcal{B}$ with respect to a fixed world frame. Then $\mathcal{B}$'s c-space is parametrized by $q = (d, \theta) \in I\!R^3$. The velocities of $\mathcal{B}$ are denoted $\dot{q} = (v, \omega)$, where $v \in I\!R^2$ and $\omega \in I\!R$ are $\mathcal{B}$'s linear and angular velocities. The velocities of $\mathcal{B}$ at q span the tangent space $T_q I\!R^3 \cong I\!R^3$. The wrenches acting on $\mathcal{B}$ are denoted $\boldsymbol{w} = (f, \tau)$, where $f \in I\!R^2$ and $\tau \in I\!R$ are the force and torque acting on $\mathcal{B}$. The wrenches acting on $\mathcal{B}$ at q span the *wrench space* $T_q^* I\!R^3 \cong I\!R^3$.

Let f_i denote the i^{th} contact force acting on $\mathcal{B}$ at a point x_i, where f_i and x_i are described in the fixed world frame ($i = 1 \ldots k$). The wrench generated by f_i is specified as follows (Figure 1). Let r_i describe the point x_i in $\mathcal{B}$'s body frame i.e., $x_i = R(\theta) r_i + d$. Let

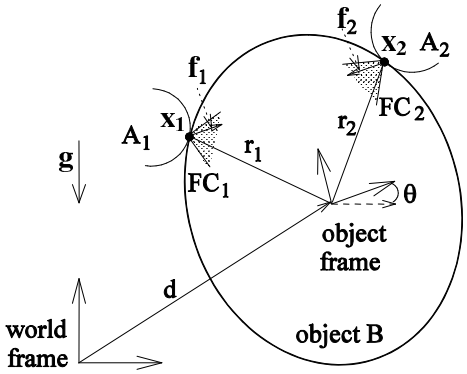

Figure 1: Basic frictional grasp notation.

$\boldsymbol{\rho}_i(\theta) = R(\theta)r_i$. The wrench induced by f_i, denoted $\boldsymbol{w}_i$, is given by

$$\boldsymbol{w}_i = \begin{pmatrix} f_i \\ \boldsymbol{\rho}_i \times f_i \end{pmatrix} \qquad i = 1 \ldots k,$$

where $\boldsymbol{\rho}_i \times f_i$ is the torque generated by f_i. The torque can also be written as $\boldsymbol{\rho}_i \times f_i = \boldsymbol{\rho}_i^T J f_i$, where $J = \begin{bmatrix} 0 & 1 \\ -1 & 0 \end{bmatrix}$. Under the Coulomb friction model f_i must lie in the friction cone: $FC_i = \{f_i\colon\ f_i^n \geq 0 \text{ and } |f_i^t| \leq \mu f_i^n\}$, where f_i^t and f_i^n are the tangent and inward normal components of f_i, and μ is the friction coefficient. The condition $f_i^n \geq 0$ expresses the constraint that f_i can only push on $\mathcal{B}$. The set of wrenches generated by the forces of FC_i span a cone based at the wrench space origin. This feasible wrench cone, denoted $\mathcal{W}_i$, is given by

$$\mathcal{W}_i = \left\{ \boldsymbol{w}_i = \begin{pmatrix} f_i \\ \boldsymbol{\rho}_i \times f_i \end{pmatrix} : f_i \in FC_i \right\} \quad i = 1 \ldots k.$$

Next we introduce notation for the gravitational wrench. Let r_c denote the position of $\mathcal{B}$'s center of mass in its body frame. Let $x_c(q)$ denote the position of r_c in the fixed world frame, $x_c(q) = R(\theta)r_c + d$. The gravitational potential energy of $\mathcal{B}$ is given by $U_g(q) = mg\boldsymbol{e}\cdot x_c(q)$, where m is $\mathcal{B}$'s mass, g is the gravitational constant, and $\boldsymbol{e}$ is the unit upward direction in the planar environment. Now let $f_g = -mg\boldsymbol{e}$ denote the gravitational force acting on $\mathcal{B}$. The gravitational wrench induced by this force, $\boldsymbol{w}_g$, is given by

$$\boldsymbol{w}_g = -\nabla U_g(q) = \begin{pmatrix} f_g \\ \boldsymbol{\rho}_c \times f_g \end{pmatrix}, \tag{1}$$

where $\boldsymbol{\rho}_c(\theta) = R(\theta)r_c$ and $\boldsymbol{\rho}_c \times f_g = \boldsymbol{\rho}_c^T J f_g$. Based on this notation, $\mathcal{B}$ is held at a feasible *equilibrium grasp* in the presence of gravity (without any other external influences) when the net wrench on $\mathcal{B}$ is zero:

$$\sum_{i=1}^{k} \boldsymbol{w}_i + \boldsymbol{w}_g = \vec{0} \quad \text{where } \boldsymbol{w}_i \in \mathcal{W}_i \text{ for } i = 1 \ldots k.$$

The equilibrium condition can also be written in terms of $f_1 \ldots f_k$ and f_g as

$$\sum_{i=1}^{k} \begin{pmatrix} f_i \\ \boldsymbol{\rho}_i \times f_i \end{pmatrix} + \begin{pmatrix} f_g \\ \boldsymbol{\rho}_c \times f_g \end{pmatrix} = \vec{0} \quad \text{where } f_i \in FC_i \text{ for } i = 1 \ldots k.$$

An equilibrium grasp is said to be *non-marginal* when the contact forces $f_1 \dots f_k$ are not all zero, such that the non-zero forces among $f_1 \dots f_k$ lie in the interior of their respective friction cones [20, 24].

2.2 Review of Force Closure

The collection of net wrenches that can be generated by k frictional contacts is the set sum $\mathcal{W}_1 + \cdots + \mathcal{W}_k$. Full force closure requires that this collection be capable of balancing any disturbance wrench as follows.

Definition 1 ([28])**.** *Let an object $\mathcal{B}$ be held in a k-contact equilibrium grasp. The grasp is **full force closure** if the set of feasible net wrenches spans the entire wrench space, $\mathcal{W}_1 + \cdots + \mathcal{W}_k = I\!R^3$.*

Full force closure guarantees that the contacts can in principle balance any disturbance wrench acting on $\mathcal{B}$. The following simple criterion determines if a given grasp arrangement is full force closure.

Theorem 1 ([20, 24, 38])**.** *A k-contact grasp of a planar object $\mathcal{B}$ is full force closure iff the contacts can establish a **non-marginal** equilibrium grasp of $\mathcal{B}$.*

It is worth mentioning that the theorem also applies to 3D grasps involving $k \geq 3$ contacts, provided that the contacts do not lie on a common spatial line [20]. Full force closure is often too conservative for grasping and fixturing applications in a gravitational field. Gravity can be thought of as a special "finger force," acting downward at $\mathcal{B}$'s center of mass. While the supporting contacts can freely adjust their forces, the gravitational force has a fixed direction and magnitude. Hence only a subset of disturbance wrenches can be balanced by the contacts. The following definition, adapted from Reuleaux [25], captures this situation.

Definition 2. *Let an object $\mathcal{B}$ be supported against gravity at a k-contact equilibrium stance. The stance is **partial force closure** if the set of feasible net wrenches, $\mathcal{W}_1 + \cdots + \mathcal{W}_k + \boldsymbol{w}_g$, spans a neighborhood about the wrench space origin.*

Note that $\mathcal{W}_1 + \cdots + \mathcal{W}_k + \boldsymbol{w}_g$ forms a semi-infinite cone based at $\boldsymbol{w}_g$ in $\mathcal{B}$'s wrench space. Partial force closure allows greater contact-placement flexibility than full force closure, since a downward restraining force is already provided by gravity. However, full/partial force closure does not specify *how* the contacts should react to a given disturbance wrench. This paper considers contacts whose reaction is governed by the following linear law.

Definition 3. *Let $\mathcal{B}$ be held at a k-contact equilibrium grasp. Let y_i^0 and f_i^0 for $i = 1 \dots k$ be the fingertip positions and preload forces at the equilibrium grasp. The fingertips satisfy **linear force-displacement laws** when they generate the contact force:*

$$f_i = -K_i(y_i - y_i^0) + f_i^0 \quad \textit{for } i = 1 \dots k, \tag{2}$$

*where y_i is the i^{th} fingertip position in the fixed world frame, and $K_i \geq 0$ is the 2×2 **i^{th} contact stiffness matrix.***

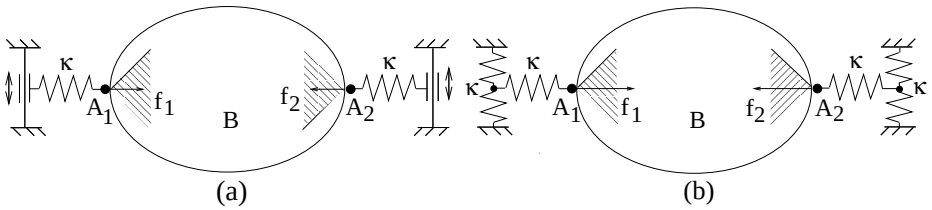

Figure 2: A full force closure grasp which is (a) not passive force closure, and (b) ceases to be passive force closure beyond a certain preload level.

The preload forces are typically generated by specifying a fixed setpoint, say z_i^0, such that $f_i^0 = -K_i(y_i^0 - z_i^0)$ for $i = 1 \ldots k$. Once the fingers are preloaded against $\mathcal{B}$, they can only *passively* react to external wrenches acting on $\mathcal{B}$ by monitoring their tip positions and generating forces according to the force-displacement law (2) [31, 37]. A notion of force closure suitable for this passive setting, adapted from Yoshikawa [38], is as follows.

Definition 4. *Let an object $\mathcal{B}$ be held in a preloaded equilibrium grasp by k contacts satisfying the linear force-displacement law (2). The grasp is* **passive force closure** *if the contacts can stably balance any external wrench in a neighborhood of the wrench space origin.*

Passive force closure ensures that when sufficiently small disturbance wrenches act on $\mathcal{B}$, the object automatically settles at a nearby equilibrium where the contacts balance the wrench. The notion of passive force closure extends to any force displacement law of the form $f_i = g_i(y_i)$, where g_i is a smooth function of the fingertip position y_i. Note that the conditions for full/partial force closure are necessary but not sufficient for passive force closure (Proposition 2.1), for the simple reason that passive force closure also accounts for the laws governing the contacts. In particular, passive force closure depends on the preload forces as illustrated in the following example.

Example 1: Consider the two-finger grasps of an ellipse depicted in Figure 2, which take place in a horizontal plane without gravity. Both grasps are full force closure. When the ellipse is grasped by the fixturing devices of Figure 2(a), the contacts satisfy linear force-displacement laws having stiffness matrices $K_1 = K_2 = \begin{bmatrix} \kappa & 0 \\ 0 & 0 \end{bmatrix}$ for some $\kappa > 0$. The resulting grasp is *not* passive force closure, since the contacts cannot resist vertical forces acting on the ellipse. Consider now the grasp of Figure 2(b), where $K_1 = K_2 = \begin{bmatrix} \kappa & 0 \\ 0 & \kappa \end{bmatrix}$ for some $\kappa > 0$. The grasp's passive force closure depends on the elastic energy stored in the compressed contacts. It is shown in Proposition 2.1 that passive force closure requires that the grasp's configuration be a strict local minimum of its total potential energy function. Beyond a certain preload level this grasp ceases to be a local minimum of its potential energy function, and the grasp is no longer passive force closure. This phenomenon is known as "coin snapping" in the grasping literature [6, 19].

This paper describes various aspects of the passive force closure set using the two-finger grasp of an ellipse as a running example. However, the ellipse has no importance here and can be replaced by any piecewise smooth object. Similarly, the two contacts can be replaced by a higher number of contacts without affecting the principle results reported in the paper. The following proposition provides a passive force closure criterion. The proposition assumes that each contact is governed by a force-displacement law induced by an elastic potential

energy $U_i(q)$ for $i = 1 \ldots k$.[1] Under this assumption the grasp's total potential energy is the sum $U(q) = \sum_{i=1}^{k} U_i(q) + U_g(q)$, where $U_g(q)$ is $\mathcal{B}$'s gravitational potential energy.

Proposition 2.1. *Let $\mathcal{B}$ be held at a preloaded equilibrium grasp by k contacts satisfying the linear force-displacement law (2). Let $U(q)$ be $\mathcal{B}$'s total potential energy. If the grasp is non-marginal and forms a non-degenerate local minimum of U, it is* **passive force closure.**

A proof of the proposition is sketched in Appendix A. The requirement that the equilibrium grasp be a non-degenerate extremum of U guarantees that all sufficiently small disturbance wrenches can be balanced at a nearby equilibrium. The requirement that the equilibrium grasp be a local minimum of U guarantees that all nearby equilibria are locally stable, and consequently that the initial equilibrium will converge to the equilibrium induced by the disturbance wrench. Without this requirement arbitrary small disturbance wrenches may result in a gross motion of $\mathcal{B}$ away from the initial equilibrium grasp (see Section 5).

3 The Passive Force Closure Set

This section characterizes the set of external wrenches that can be stably balanced by a grasp whose contacts satisfy linear force-displacement laws. This collection of wrenches, called the *passive force closure set,* is characterized in two stages. First we characterize the set of external wrenches that can be stably balanced in a manner consistent with the friction cone constraints. Then we derive a global criterion which ensures convergence of the unperturbed equilibrium to the equilibrium induced by a given external wrench. The collection of external wrenches satisfying these two conditions forms the passive force closure set.

3.1 Local Conditions for the Passive Force Closure Set

Let $\mathcal{B}$ be held by k contacts at a passive force-closure grasp configuration q_0. Now let a collection of fixed forces act at various points of $\mathcal{B}$ and generate a net disturbance wrench $\boldsymbol{w}_{ext}$. We wish to determine which disturbance wrenches can be balanced at a locally stable equilibrium satisfying the friction cone constraints. We first characterize this requirement in $\mathcal{B}$'s c-space, then obtain the collection of permissible disturbance wrenches by a suitable mapping from $\mathcal{B}$'s c-space to its wrench space.

The collection of contact forces satisfying the friction cone constraints can be characterized in $\mathcal{B}$'s c-space as follows. The position of the i^{th} contact in the fixed world frame is $x_i(q) = R(\theta)r_i + d$, where $q = (d, \theta)$. The collection of $\mathcal{B}$'s configurations at which the k contact forces lie in the *interior* of their friction cones, denoted $\mathcal{FQ}$, is considered below. As long as $q \in \mathcal{FQ}$ the fingertips do not break contact or slip with respect to $\mathcal{B}$. For these configurations we may write $y_i = x_i(q)$, where y_i is the i^{th} fingertip position for $i = 1 \ldots k$. Substituting $y_i = x_i(q)$ in (2) gives the contact reaction forces:

$$f_i(q) = -K_i\big(x_i(q) - y_i^0\big) + f_i^0 \quad \text{for } i = 1 \ldots k. \tag{3}$$

We can now express the friction cone constraints as a set $\mathcal{FQ}$ in $\mathcal{B}$'s c-space. This set is given by the intersection $\mathcal{FQ} = \cap_{i=1}^{k} \mathcal{FQ}_i$, where $\mathcal{FQ}_i = \{q : f_i(q) \in \mathsf{int}(FC_i)\}$ and $\mathsf{int}(\cdot)$

[1] This assumption requires that the contacts be preloaded against $\mathcal{B}$ without breakage or slippage.

denotes set interior. Let us introduce notation for the friction cones. Let t_i and n_i be the unit tangent and normal to $\mathcal{B}$ at r_i, both described in $\mathcal{B}$'s body frame, such that n_i points into $\mathcal{B}$. The description of t_i and n_i in the fixed world frame is $R(\theta)t_i$ and $R(\theta)n_i$. Based on this notation $f_i^t(q) = f_i(q)\cdot R(\theta)t_i$, $f_i^n(q) = f_i(q)\cdot R(\theta)n_i$, and $\mathcal{FQ}$ is given by

$$\mathcal{FQ} = \bigcap_{i=1}^{k} \{q:\ \ f_i(q)\cdot R(\theta)n_i > 0 \quad \text{and} \quad |f_i(q)\cdot R(\theta)t_i| < \mu f_i(q)\cdot R(\theta)n_i\}, \tag{4}$$

where $f_i(q)$ is specified in (3). The set $\mathcal{FQ}$ is the collection of $\mathcal{B}$'s configurations at which the contacts can balance a candidate $\boldsymbol{w}_{ext}$ without incurring contact breakage or slippage.

Next we establish a local stability criterion for an equilibrium induced by $\boldsymbol{w}_{ext}$. The criterion is based on the general fact that a damped mechanical system governed by a potential energy function converges to the local minima of the potential function [15].[2] Dissipation arises in our system from several sources, such as damping within the finger mechanisms and viscoelastic effects at the contacts [14, p. 302-308]. In our setup $\boldsymbol{w}_{ext}$ can be written in terms of a potential function, $U_{ext}(q)$, as follows. Consider the situation where $\boldsymbol{w}_{ext}$ is generated by a single force, f_{ext}, which acts on $\mathcal{B}$ at a point r_{ext} (the case were $\boldsymbol{w}_{ext}$ is generated by multiple forces gives a similar potential function). Let $x_{ext}(q) = R(\theta)r_{ext} + d$ denote the position of r_{ext} in the fixed world frame. Then $U_{ext}(q) = -x_{ext}(q)\cdot f_{ext}$, and the wrench induced by f_{ext} is the negated gradient $\boldsymbol{w}_{ext} = -\nabla U_{ext}(q) = (f_{ext}, \boldsymbol{\rho}_{ext}(\theta) \times f_{ext})$, where $\boldsymbol{\rho}_{ext}(\theta) = R(\theta)r_{ext}$ and $\boldsymbol{\rho}_{ext} \times f_{ext} = \boldsymbol{\rho}_{ext}^T J f_{ext}$. Based on this observation, the total influences on $\mathcal{B}$ are captured by the potential function:

$$V(q) = \sum_{i=1}^{k} U_i(q) + U_g(q) + U_{ext}(q),$$

where $\sum_{i=1}^{k} U_i$ is the elastic energy stored at the contacts, and U_g is the gravitational potential energy. Any equilibrium induced by $\boldsymbol{w}_{ext}$ is an extremum of V satisfying the condition:

$$\sum_{i=1}^{k} \begin{pmatrix} f_i \\ \boldsymbol{\rho}_i(\theta) \times f_i(q) \end{pmatrix} + \begin{pmatrix} f_g \\ \boldsymbol{\rho}_c(\theta) \times f_g \end{pmatrix} + \begin{pmatrix} f_{ext} \\ \boldsymbol{\rho}_{ext}(\theta) \times f_{ext} \end{pmatrix} = \vec{0} \quad f_i \in FC_i \text{ for } i = 1 \ldots k.$$

An equilibrium induced by $\boldsymbol{w}_{ext}$ is locally stable if it is a non-degenerate local minimum of V i.e., if $D^2V(q) > 0$. The set of $\mathcal{B}$'s configurations satisfying local stability, denoted $\mathcal{PQ}$, is given by $\mathcal{PQ} = \{q : \lambda_{min}\big(D^2V(q)\big) > 0\}$ where λ_{min} denotes minimal eigenvalue.

We now express the set $\mathcal{PQ}$ as a function of the grasp's geometry and the contact forces. The formula for D^2V has been obtained by several authors (e.g. [20]), and its derivation is summarized in Appendix B. This formula is given by

$$D^2V(q) = \sum_{i=1}^{k} \begin{bmatrix} K_i & K_i J\boldsymbol{\rho}_i \\ (J\boldsymbol{\rho}_i)^T K_i & (J\boldsymbol{\rho}_i)^T K_i J\boldsymbol{\rho}_i + f_i(q)\cdot\boldsymbol{\rho}_i \end{bmatrix} + \begin{bmatrix} O & 0 \\ 0^T & \boldsymbol{\rho}_c\cdot f_g \end{bmatrix} + \begin{bmatrix} O & 0 \\ 0^T & \boldsymbol{\rho}_{ext}\cdot f_{ext} \end{bmatrix},$$

where K_i is the i^{th} contact stiffness matrix, $J = \begin{bmatrix} 0 & 1 \\ -1 & 0 \end{bmatrix}$, and O is a 2×2 matrix of zeroes. The first summand is the classical grasp stiffness matrix induced by the reactive finger forces.

[2] The potential function extrema are required to be non-degenerate, and convergence to the local minima is from almost all initial points [15].

The formula for D^2V can also be written as the sum:

$$D^2V(q) = \sum_{i=1}^{k} \begin{bmatrix} K_i & K_i J\boldsymbol{\rho}_i \\ (J\boldsymbol{\rho}_i)^T K_i & (J\boldsymbol{\rho}_i)^T K_i J\boldsymbol{\rho}_i \end{bmatrix} + \begin{bmatrix} O & 0 \\ 0^T & \sum_{i=1}^{k} f_i(q)\cdot\boldsymbol{\rho}_i + \boldsymbol{\rho}_c\cdot f_g + \boldsymbol{\rho}_{ext}\cdot f_{ext} \end{bmatrix},$$

such that the first summand is always positive semi-definite. It follows that any instability is generated by destabilizing torques acting along $\mathcal{B}$'s θ coordinate. Based on the formula for D^2V, the expression for the set $\mathcal{PQ}$ is as follows.

Lemma 3.1. *Let a planar object $\mathcal{B}$ be held by k contacts satisfying the linear force-displacement law (3), such that $\sum_{i=1}^{k} K_i > 0$. The set of $\mathcal{B}$'s locally stable equilibrium configurations, $\mathcal{PQ} = \{q : \lambda_{min}\big(D^2V(q)\big) > 0\}$, is given by*

$$\mathcal{PQ} = \Big\{q : P_{22} - P_{12}^T P_{11}^{-1} P_{12} + \sum_{i=1}^{k} f_i(q)\cdot(\boldsymbol{\rho}_i - \boldsymbol{\rho}_{ext}) + (\boldsymbol{\rho}_c - \boldsymbol{\rho}_{ext})\cdot f_g > 0\Big\}, \tag{5}$$

where $P_{11} = \sum_{i=1}^{k} K_i$, $P_{12} = \sum_{i=1}^{k} K_i J\boldsymbol{\rho}_i$, $P_{22} = \sum_{i=1}^{k} (J\boldsymbol{\rho}_i)^T K_i J\boldsymbol{\rho}_i$ ($\boldsymbol{\rho}_i, \boldsymbol{\rho}_c, \boldsymbol{\rho}_{ext}$ depend on θ).

The proof of the lemma appears in Appendix B. The lemma is based on the fact that planar grasps possess a special point, called the *center of compliance,* such that when $\mathcal{B}$'s origin is selected at this point the grasp's stiffness matrix becomes diagonal [20]. The term $P_{22} - P_{12}^T P_{11}^{-1} P_{12}$ is the grasp's rotational stiffness about its center of compliance. To further interpret the lemma, assume a horizontal environment without gravity. Since $f_{ext} = -\sum_{i=1}^{k} f_i(q)$ at the equilibrium induced by f_{ext}, the inequality (5) can be written as $P_{22} - P_{12}^T P_{11}^{-1} P_{12} + \sum_{i=1}^{k} f_i(q)\cdot\boldsymbol{\rho}_i + f_{ext}\cdot\boldsymbol{\rho}_{ext} > 0$. If one approximates the contact forces by the preload forces, $f_i \cong f_i^0$ for $i = 1 \ldots k$, the inequality becomes $P_{22} - P_{12}^T P_{11}^{-1} P_{12} + \sum_{i=1}^{k} f_i^0\cdot\boldsymbol{\rho}_i + f_{ext}\cdot\boldsymbol{\rho}_{ext} > 0$. It follows that the preload forces can destabilize the grasp when $\sum_{i=1}^{k} f_i^0\cdot\boldsymbol{\rho}_i < 0$ (Example 1). Moreover, the destabilizing effect of f_{ext} occurs when $f_{ext}\cdot\boldsymbol{\rho}_{ext} < 0$, and is thus similar to the destabilizing role of the preload forces.

We now map the set $\mathcal{FQ}\cap\mathcal{PQ}$ from $\mathcal{B}$'s c-space to its wrench space. When a candidate $\boldsymbol{w}_{ext}$ acts on $\mathcal{B}$ at a configuration q, the net reaction wrench is given by $\boldsymbol{w}(q) = \sum_{i=1}^{k} \boldsymbol{w}_i(q) + \boldsymbol{w}_g(q)$. This reaction wrench can be interpreted as a mapping from c-space to wrench space. The image of $\mathcal{FQ}\cap\mathcal{PQ}$ under $-\boldsymbol{w}(q)$, denoted $\mathcal{W}_{ext}$, gives the set of external wrenches that can be balanced by permissible finger forces at a locally stable equilibrium. The expressions characterizing $\mathcal{W}_{ext}$ are as follows.

Proposition 3.2. *Let a planar object $\mathcal{B}$ be held in a passive force-closure grasp by k contacts satisfying the linear force-displacement law* (3)*. The set of external wrenches that can be balanced by the contacts at a locally stable equilibrium is given by*

$$\mathcal{W}_{ext} = \left\{ -\left(\sum_{i=1}^{k} \begin{pmatrix} f_i(q) \\ \boldsymbol{\rho}_i(\theta)\times f_i(q) \end{pmatrix} - mg\begin{pmatrix} \boldsymbol{e} \\ \boldsymbol{\rho}_c(\theta)\times\boldsymbol{e} \end{pmatrix}\right) : q = \begin{pmatrix} d \\ \theta \end{pmatrix} \in \mathcal{FQ}\cap\mathcal{PQ} \right\},$$

where $\mathcal{FQ}$ is specified in (4)*, and $\mathcal{PQ} = \{q : \lambda_{min}\big(D^2V(q)\big) > 0\}$ is specified in* (5)*.*

Note that the contact positions and preload forces appear as parameters in the expressions defining $\mathcal{W}_{ext}$. In future research we plan to use these parameters for grasp and locomotion

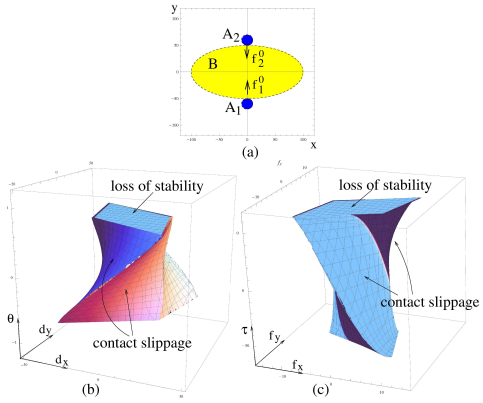

Figure 3: (a) A preloaded two-contact grasp of an ellipse. (b) The set $\mathcal{FQ} \cap \mathcal{PQ}$ of the locally feasible equilibrium configurations. (c) The corresponding set of wrenches $\mathcal{W}_{ext}$.

synthesis (see conclusion). The boundary of $\mathcal{W}_{ext}$ consists of external wrenches that generate an imminent contact slippage/breakage, or induce an equilibrium grasp which is about to become unstable. These two possibilities are experimentally verified in Section 5.

Example 2: Figure 3(a) depicts a two-finger grasp of an ellipse which lies in a horizontal plane without gravity. The ellipse's minor and major axes have lengths of 100 and 200 mm. The two fingers obey linear contact laws with contact stiffness matrices $K_i = \begin{bmatrix} 0.14 & 0 \\ 0 & 0.11 \end{bmatrix}$ for $i = 1, 2$, measured in N/mm. The grasp is preloaded along the ellipse's minor axis with forces $f_1^0 = (0, 5.8)$ and $f_2^0 = (0, -5.8)$ N.[3] The set $\mathcal{FQ} \cap \mathcal{PQ}$ for this grasp is depicted in Figure 3(b), while its wrench space image, $\mathcal{W}_{ext}$, is depicted in Figure 3(c). The side facets of $\mathcal{FQ} \cap \mathcal{PQ}$ belong to $\mathcal{FQ}$ and correspond to contact slippage or breakage. The top and bottom facets of $\mathcal{FQ} \cap \mathcal{PQ}$ belong to $\mathcal{PQ}$ and correspond to imminent loss of stability. The position of the latter facets is consistent with our earlier observation that any instability in $D^2V(q)$ occurs along $\mathcal{B}$'s θ coordinate.

3.2 Global Condition for the Passive Force Closure Set

By construction, every $\boldsymbol{w}_{ext} \in \mathcal{W}_{ext}$ can be balanced at a locally stable equilibrium, q_1, satisfying the friction cone constraints. However, the initial unperturbed equilibrium at q_0 need not converge to q_1. To derive a global convergence criterion of q_0 to q_1, we first compute all possible equilibria induced by $\boldsymbol{w}_{ext}$ and determine their stability type.

[3]The stiffness matrices and preload forces match the experimental setup discussed in Section 5.

Lemma 3.3 (Equilibrium Solutions)**.** *Let a planar object $\mathcal{B}$ be grasped by k contacts satisfying the linear contact law (3), such that $\sum_{i=1}^{k} K_i > 0$. Let $\mathcal{W}_{ext} = \{-\boldsymbol{w}(q) : q \in \mathcal{FQ} \cap \mathcal{PQ}\}$. Then every $\boldsymbol{w}_{ext} \in \mathcal{W}_{ext}$ acting on $\mathcal{B}$ induces either two or four equilibrium grasps.*

Proof: Let $\boldsymbol{w}_{ext}$ be generated by a single force f_{ext}, so that $\boldsymbol{w}_{ext} = (f_{ext}, \boldsymbol{\rho}_{ext} \times f_{ext})$ (a similar proof holds when $\boldsymbol{w}_{ext}$ is generated by multiple forces). The force part of the equilibrium induced by f_{ext} is: $\sum_{i=1}^{k} f_i(q) + f_g + f_{ext} = \vec{0}$. Substituting for $f_i(q)$ according to (3) gives $\sum_{i=1}^{k} \big(f_i^0 - K_i(x_i(q) - y_i^0)\big) + f_g + f_{ext} = \vec{0}$ for $i = 1 \ldots k$. Since $\sum_{i=1}^{k} f_i^0 + f_g = \vec{0}$ at q_0, the force-balance equation becomes $f_{ext} - \sum_{i=1}^{k} K_i(x_i(q) - y_i^0) = \vec{0}$. Substituting $x_i(q) = \boldsymbol{\rho}_i(\theta) + d$ gives $f_{ext} - \sum_{i=1}^{k} K_i(\boldsymbol{\rho}_i(\theta) + d - y_i^0) = \vec{0}$. Next we solve for $\mathcal{B}$'s equilibrium position, d, as a function of $\mathcal{B}$'s orientation θ. Using the notation $P = \sum_{i=1}^{k} K_i$ and the assumption that $P > 0$, the solution for $d(\theta)$ is given by

$$d(\theta) = P^{-1}\big(f_{ext} - \sum_{i=1}^{k} K_i(\boldsymbol{\rho}_i(\theta) - y_i^0)\big). \tag{6}$$

The torque-part of the equilibrium induced by f_{ext} is the scalar equation: $\sum_{i=1}^{k} \boldsymbol{\rho}_i \times f_i + \boldsymbol{\rho}_c \times f_g + \boldsymbol{\rho}_{ext} \times f_{ext} = 0$. Substituting for $f_i(q)$ according to (3) gives $\sum_{i=1}^{k} \boldsymbol{\rho}_i \times \big(f_i^0 - K_i(\boldsymbol{\rho}_i + d - y_i^0)\big) + \boldsymbol{\rho}_c \times f_g + \boldsymbol{\rho}_{ext} \times f_{ext} = 0$. Substituting for $d(\theta)$ and using the identity $\boldsymbol{\rho} \times v = \boldsymbol{\rho}^T J v$, we obtain the torque-balance equation:

$$\sum_{i=1}^{k} \boldsymbol{\rho}_i^T J\big(f_i^0 - K_i\big(\boldsymbol{\rho}_i + P^{-1}\big(f_{ext} - \sum_{j=1}^{k} K_j(\boldsymbol{\rho}_j - y_j^0)\big) - y_i^0\big)\big) + \boldsymbol{\rho}_c^T J f_g + \boldsymbol{\rho}_{ext}^T J f_{ext} = 0.$$

Let $A_i = JK_i$, $B_{ij} = JK_iP^{-1}K_j$, and $\boldsymbol{c}_i = J\big(f_i^0 - K_i(P^{-1}(f_{ext} + \sum_{j=1}^{k} K_j y_j^0) - y_i^0)\big)$ for $i = 1 \ldots k$ and $j = 1 \ldots k$. Note that A_i, B_{ij}, and $\boldsymbol{c}_i$ are all constants. Substituting these constants in the torque-balance equation gives

$$\sum_{i=1}^{k} \left\{ \sum_{j=1}^{k} \boldsymbol{\rho}_i(\theta)^T B_{ij} \boldsymbol{\rho}_j(\theta) - \boldsymbol{\rho}_i(\theta)^T A_i \boldsymbol{\rho}_i(\theta) + \boldsymbol{\rho}_i(\theta)^T \boldsymbol{c}_i \right\} + \boldsymbol{\rho}_c^T(\theta) J f_g + \boldsymbol{\rho}_{ext}^T(\theta) J f_{ext} = 0. \tag{7}$$

In this equation $\boldsymbol{\rho}_i(\theta) = R(\theta) r_i$ $(i = 1 \ldots k)$, $\boldsymbol{\rho}_c = R(\theta) r_c$, and $\boldsymbol{\rho}_{ext} = R(\theta) r_{ext}$. Since $R(\theta) = \begin{bmatrix} \cos(\theta) & -\sin(\theta) \\ \sin(\theta) & \cos(\theta) \end{bmatrix}$, eq. (7) is quadratic in $\sin(\theta)$ and $\cos(\theta)$. Substituting the identities $\sin(\theta) = 2z/(1+z^2)$ and $\cos(\theta) = (1-z^2)/(1+z^2)$ gives a fourth-order polynomial in $z = \tan(\theta/2)$. As the complex roots of the latter polynomial occur in conjugate pairs, it can have zero, two, or four real roots. Each real root, z_i for $1 \le i \le 4$, determines an equilibrium solution $\big(d(\theta_i), \theta_i\big)$, where $\theta_i = 2\arctan(z_i)$ and $d(\theta_i)$ is obtained from (6). Finally, since $\boldsymbol{w}_{ext} \in \mathcal{W}_{ext}$, it induces at least one equilibrium. Hence $\boldsymbol{w}_{ext}$ induces either two or four equilibria. □

Some intuition for the number of equilibria is as follows. The equilibrium solutions are extrema of $\mathcal{B}$'s total potential energy function, $V(q)$. Since $\mathcal{B}$'s c-space is topologically equivalent to a solid torus, the extrema of $V(q)$ must appear in stable and unstable pairs. Hence there must be an even number of extrema. Now observe that $V(q)$ is quadratic in d and in $(\cos\theta, \sin\theta)$, where $q = (d, \theta)$. The extremum condition, $\nabla V(q) = \vec{0}$, gives three scalar equations which are linear in d and linear in $(\cos\theta, \sin\theta)$. One can use the first two equations

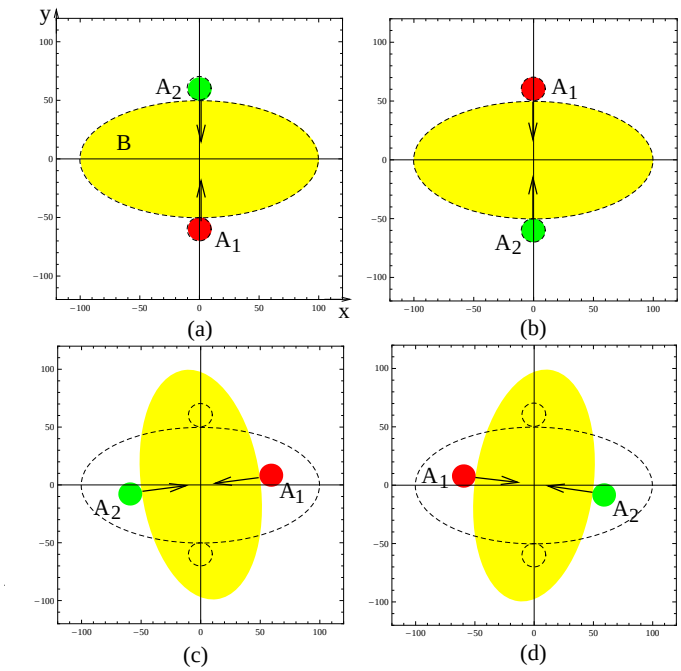

Figure 4: The four equilibria associated with the preloaded two-finger grasp of Example 2: (a)-(b) q_1 and q_2 are locally stable, (c)-(d) q_3 and q_4 are unstable saddles.

to express d as a linear function of $(\cos\theta, \sin\theta)$. When this expression is substituted into the third equation, one obtains a quadratic equation in $(\cos\theta, \sin\theta)$. This gives a fourth-order polynomial in θ whose solutions are the four possible equilibria.

Example 3: Consider the two-finger grasp of the ellipse discussed in Example 2. The grasp is preloaded along the ellipse's minor axis with forces $f_1^0 = (0, 5.8)$ and $f_2^0 = (0, -5.8)$ N, and the contact stiffness matrices are $K_i = \begin{bmatrix} 0.14 & 0 \\ 0 & 0.11 \end{bmatrix}$ for $i = 1, 2$, measured in N/ mm. Even without any disturbance wrench, $\mathcal{B}$ has *four* possible equilibria depicted in Figure 4. The equilibria lie at the configurations $q_1 = (0, 0, 0)$, $q_2 = (0, 0, -\pi)$, $q_3 = (0, 0, -1.43)$, and $q_4 = (0, 0, 1.43)$, where $\mathcal{B}$'s position and orientation is measured in mm and radians. The equilibrium q_1 is the nominal grasp depicted in Figure 4(a). At q_2 the contacts switch positions (Figure 4(b)), and the finger forces are $f_1 = -K_1\Delta x_1 + f_1^0 = (0, -5.42)$ and $f_2 = -K_2\Delta x_2 + f_2^0 = (0, 5.42)$ N. At q_3 the contacts are located at $x_1 = (49.54, 6.79)$ and $x_2 = (-49.54, -6.79)$ (Figure 4(c)), and the finger forces are given by $f_1 = -K_1\Delta x_1 + f_1^0 = (-6.95, -0.95)$ and $f_2 = -K_2\Delta x_2 + f_2^0 = (6.95, 0.95)$ N. At q_4 the contacts lie at $x_1 = (-49.54, 6.79)$ and $x_2 = (49.54, -6.79)$ (Figure 4(d)), and the finger forces are $f_1 = -K_1\Delta x_1 + f_1^0 = (6.95, -0.95)$ and $f_2 = -K_2\Delta x_2 + f_2^0 = (-6.95, 0.95)$ N. As discussed in Lemma 3.4, the equilibria q_1 and q_2 are locally stable while q_3 and q_4 are unstable saddles. Note that q_3 and q_4 require a sufficiently large friction coefficient to be physically feasible.

The next lemma characterizes the stability type of the equilibria induced by $\boldsymbol{w}_{ext} \in \mathcal{W}_{ext}$.

Lemma 3.4 (Equilibrium Classification)**.** *Let a planar object $\mathcal{B}$ be grasped by k contacts satisfying the linear contact law (3), such that $\sum_{i=1}^{k} K_i > 0$. When $\boldsymbol{w}_{ext} \in \mathcal{W}_{ext}$ induces two equilibria, one is locally stable while the other is an unstable saddle. When $\boldsymbol{w}_{ext} \in \mathcal{W}_{ext}$ induces four equilibria, two are locally stable while the other two are unstable saddles.*

The proof of the lemma is based on Morse theory and appears in Appendix C. As discussed above, $\mathcal{B}$'s motions under the influence of $\boldsymbol{w}_{ext}$ are governed by the potential function $V(q) = \sum_{i=1}^{k} U_i(q) + U_g(q) + U_{ext}(q)$. The equilibria induced by $\boldsymbol{w}_{ext}$ are the critical points of V, and their stability is determined by the type of critical points (a local minimum, a saddle, or a local maximum). We now turn to the task of delineating the basin of attraction of the local minima induced by $\boldsymbol{w}_{ext}$. First consider the case where $\boldsymbol{w}_{ext}$ induces two equilibria. Let q_1 and q_2 denote these two equilibria, such that q_1 is stable and q_2 unstable. Then V has a local minimum at q_1 and a saddle at q_2. Moreover, it can be verified that $V(q_1) < V(q_2)$. Based on Morse theory reviewed in Appendix C, the sub-level set $\{q : V(q) \leq V(q_2)\}$ is topologically equivalent to a solid ball in $\mathcal{B}$'s c-space. The boundary of this ball, a topological sphere, passes through q_2. Since V represents the net potential energy of $\mathcal{B}$, by conservation of energy any initial zero-velocity configuration within this sub-level set converges to q_1. Convergence to q_1 in the sub-level sets beyond $V(q_2)$ is guaranteed only from almost all initial points. For simplicity and symmetry with the four-equilibrium case discussed below, we define the basin of attraction of q_1, denoted $\mathsf{Basin}(q_1)$, as the set $\mathsf{Basin}(q_1) = \{q : V(q) \leq V(q_2)\}$.

Consider now the case where $\boldsymbol{w}_{ext}$ induces four equilibria. Let q_1 and q_2 denote the stable equilibria, let q_3 and q_4 denote the unstable equilibria. Then V has local minima at q_1 and q_2 and saddles at q_3 and q_4. The following lemma specifies the relative value of V at the four equilibria and provides a separation criterion for the basins of q_1 and q_2.

Lemma 3.5. *Let a planar object $\mathcal{B}$ be grasped by k contacts satisfying the linear contact law (3), such that $\sum_{i=1}^{k} K_i > 0$. Let $\boldsymbol{w}_{ext} \in \mathcal{W}_{ext}$ induce four equilibria, q_i for $i = 1 \ldots 4$, such that q_1 and q_2 are local minima while q_3 and q_4 are saddles of $V(q)$.*
Then $V(q_1), V(q_2) < V(q_3) \leq V(q_4)$. In particular, the sub-level set $\{q : V(q) \leq V(q_3)\}$ consists of two topological solid balls touching at q_3 and separated by the fixed-θ planes passing through q_3 and q_4 (Figure 5).

The proof of the lemma is based on Morse theory and appears in Appendix C.

Example 4: Figure 5(a) shows the level surface $V(q) = V(q_3)$ for the preloaded two-finger grasp of the ellipse discussed in Example 2 (see Figure 3(a)). The level surface shown in Figure 5(a) corresponds to the case where no external load acts on $\mathcal{B}$. In this case $q_1 = q_0$, and the level surface $V(q) = V(q_3)$ consists of two spheres meeting at the saddles q_3 and q_4. The set $\mathsf{Basin}(q_1)$ is the solid ball at the center of the figure. Note that this basin is bounded by the fixed-θ planes passing through the saddles q_3 and q_4.

The two solid balls comprising the sub-level set $V(q) \leq V(q_3)$ form the basins of attraction, $\mathsf{Basin}(q_1)$ and $\mathsf{Basin}(q_2)$, of the local minima at q_1 and q_2. Let θ_i be the θ-coordinate of the equilibrium q_i for $i = 1 \ldots 4$. Then the two basins of attraction are given by

$$\mathsf{Basin}(q_i) = \left\{ q = \begin{pmatrix} d \\ \theta \end{pmatrix} : V(q) \leq V(q_3) \quad \text{and} \quad \theta \in \begin{cases} [\theta_3, \theta_4] & \text{if } \theta_i \in [\theta_3, \theta_4] \\ [\theta_4, \theta_3] & \text{if } \theta_i \in [\theta_4, \theta_3] \end{cases} \right\} \text{ for } i = 1, 2, \qquad (8)$$

where $[\theta_3, \theta_4]$ and $[\theta_4, \theta_3]$ are complementary intervals within $[-\pi, \pi]$, measured modulo 2π. We now give a concise characterization of the passive force closure set. Denote by $\overline{\mathcal{W}}_{ext}$ the passive force closure set associated with a nominal equilibrium grasp at q_0. The following theorem is a key result of this paper.

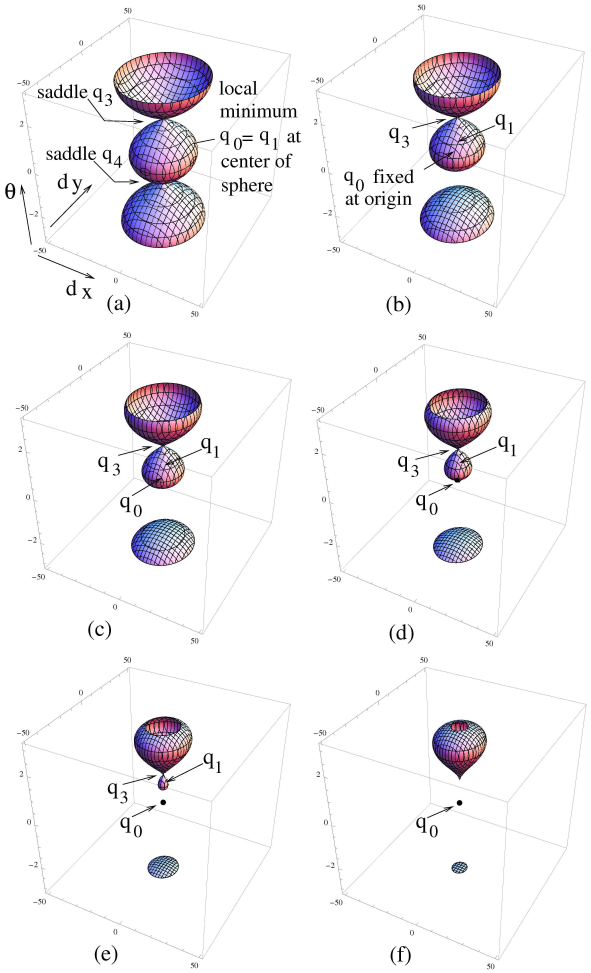

Figure 5: The level surface $V(q) = V(q_3)$ of the grasp of Example 2 for (a) $\tau_{ext} = 0$, (b) $\tau_{ext} = 20$, (c) $\tau_{ext} = 40$, (d) $\tau_{ext} = 60$, (e) $\tau_{ext} = 80$, and (f) $\tau_{ext} = 90$ $\mathsf{N}\cdot$mm.

Theorem 2 (Passive Force Closure Set)**.** *Let $\mathcal{C}(\boldsymbol{w}_{ext})$ be the discrete set of equilibria induced by $\boldsymbol{w}_{ext}$ i.e., the equilibrium solutions $(d(\theta_i), \theta_i)$ for $1 \leq i \leq 4$. Then $\boldsymbol{w}_{ext}$ lies in $\overline{\mathcal{W}}_{ext}$ if one of the locally stable equilibria in $\mathcal{C}(\boldsymbol{w}_{ext})$ satisfies the friction cone constraints, such that its basin of attraction contains the initial unperturbed equilibrium:*

$$\overline{\mathcal{W}}_{ext} = \big\{ \boldsymbol{w}_{ext} : \exists q_i \in \mathcal{C}(\boldsymbol{w}_{ext}) \quad q_i \in \mathcal{F}Q \cap \mathcal{P}Q \quad \textit{and} \quad q_0 \in \mathsf{Basin}(q_i) \big\}, \tag{9}$$

where $\mathsf{Basin}(q_i)$ *is specified in* (8).

Note that $\mathcal{C}(\boldsymbol{w}_{ext})$ always contains at least one locally stable equilibrium, $q_i \in \mathcal{F}P$. This q_i may not satisfy the friction cone constraints, and is therefore required to lie in $\mathcal{F}Q \cap \mathcal{P}Q$. The criteria specified in (9) can be evaluated for a given $\boldsymbol{w}_{ext}$ as follows. First determine the number and stability type of the equilibria induced by $\boldsymbol{w}_{ext}$. When $\boldsymbol{w}_{ext}$ induces two equilibria, a local minimum q_1 and a saddle q_2, the criterion $q_0 \in \mathsf{Basin}(q_1)$ becomes the inequality $V(q_0) \leq V(q_2)$. When $\boldsymbol{w}_{ext}$ induces four equilibria, two local minima are located at q_1 and q_2, while two saddles are located at q_3 and q_4. In this case the sub-level set $V(q) \leq V(q_3)$ consists of two solid balls centered at q_1 and q_2. The fixed-θ planes passing through q_3 and q_4 separate the two balls, and the criterion $q_0 \in \mathsf{Basin}(q_i)$ consists of the inequality $V(q_0) \leq V(q_3)$ as well as the test $\theta_0, \theta_i \in [\theta_3, \theta_4] \bmod 2\pi$ or $\theta_0, \theta_i \in [\theta_4, \theta_3] \bmod 2\pi$ $(i = 1, 2)$.

Example 5: This example illustrates the basin criterion, $q_0 \in \mathsf{Basin}(q_1)$, for the two-finger grasp of the ellipse discussed in Example 2. Figure 5 depicts the level-surface $V(q) = V(q_3)$ for a pure disturbance torque, τ_{ext}, which acts about the ellipse's center (such a torque can be modeled as two antiparallel forces arranged symmetrically about the ellipse's center). The initial equilibrium q_0 is fixed at the c-space origin for all values of τ_{ext}. The level surface $V(q) = V(q_3)$ corresponding to $\tau_{ext} = 0$ is depicted in Figure 5(a). In this case $q_1 = q_0$, and $\mathsf{Basin}(q_1)$ is the solid ball centered at q_1. The level surface $V(q) = V(q_3)$ for $\tau_{ext} = 20, 40, 60$ $\mathsf{N}\cdot\mathrm{mm}$ is depicted in Figures 5(b)-(d). Note that the solid ball associated with $\mathsf{Basin}(q_1)$ shrinks as τ_{ext} increases, but q_0 still lies inside $\mathsf{Basin}(q_1)$ for $\tau_{ext} = 20, 40, 60$ $\mathsf{N}\cdot\mathrm{mm}$. When τ_{ext} reaches 80 $\mathsf{N}\cdot\mathrm{mm}$, the level surface $V(q) = V(q_3)$ no longer contains the initial equilibrium q_0 (Figure 5(e)). The criterion $q_0 \in \mathsf{Basin}(q_1)$ no longer holds true, and $\tau_{ext} = 80$ $\mathsf{N}\cdot\mathrm{mm}$ therefore lies outside the passive force closure set of q_0. Finally, when τ_{ext} reaches 90 $\mathsf{N}\cdot\mathrm{mm}$ the sphere associated with $\mathsf{Basin}(q_1)$ completely vanishes (Figure 5(f)). This event corresponds to a decrease in the number of possible equilibria from four to two.[4]

3.3 Summarizing Examples

Let us illustrate the passive force closure set criteria on the two-finger grasp of the ellipse discussed in Example 2. Recall that the ellipse lies in a horizontal plane without gravity and is preloaded along its minor axis. Also recall that the two fingers obey linear contact laws with contact stiffness matrices $K_i = \left[\begin{smallmatrix} 0.14 & 0 \\ 0 & 0.11 \end{smallmatrix}\right]$ for $i = 1, 2$. We consider two preload levels. For each preload level, we apply external forces at $\mathcal{B}$'s point $r_{ext} = (20, 0)$ mm along a fixed direction aligned with the world frame y axis. The friction coefficient at the contacts is assumed to be $\mu = 0.5$.

[4]This is a *fold bifurcation* event, where the stable equilibrium q_1 meets the unstable equilibrium q_3 and the two annihilate each other.

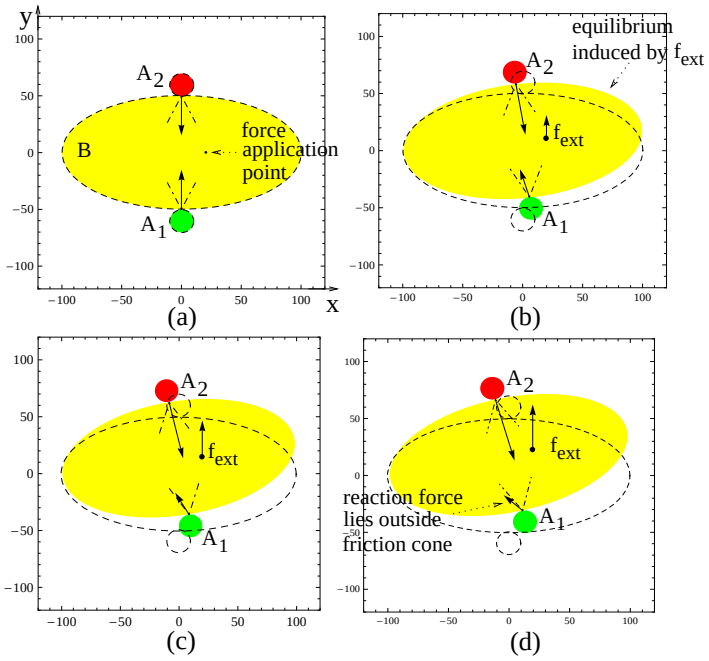

Figure 6: (a) The initial equilibrium grasp preloaded with ±3.5 N. (b)-(c) The stable equilibrium due to $\|f_{ext}\| = 2$ N and $\|f_{ext}\| = 3$ N. (d) The stable equilibrium corresponding to $\|f_{ext}\| = 4$ N violates the friction cone constraints.

Example 6: First consider a preloading of the ellipse with forces of ±3.5 N. For this preload level the initial unperturbed grasp contains only two equilibria—a stable equilibrium $q_1 = q_0$ depicted in Figure 6(a), and an unstable equilibrium at a 180° rotation of $\mathcal{B}$. The grasp's total potential energy at q_0 is $V(q_0) = 350.0$ Joules. Since f_{ext} is orthogonal to $x_{ext}(q_0) = r_{ext}$, $U_{ext}(q_0) = -x_{ext}(q_0) \cdot f_{ext} = 0$. Hence $V(q_0)$ remains constant for the external forces applied in this example. We now apply external forces of magnitudes $\|f_{ext}\| = 2$, 3, and 4 N. Each of these forces induces two equilibria—a stable equilibrium $q_1 \in \mathcal{PQ}$, and an unstable equilibrium q_2. For each of these forces, one must verify that $q_1 \in \mathcal{FQ}$ and $q_0 \in \mathsf{Basin}(q_1)$. The equilibrium q_1 induced by $\|f_{ext}\| = 2$ N is depicted in Figure 6(b). Note that $\mathcal{B}$ shifts upward and rotates in response to this force, but the contact reaction forces still lie within the friction cones. For this external force $V(q_2) = 772.7$. Since $V(q_0) < V(q_2)$, q_0 lies in $\mathsf{Basin}(q_1)$. The equilibrium q_1 induced by $\|f_{ext}\| = 3$ N is depicted in Figure 6(c). This equilibrium still satisfies the friction cone constraints. Similarly $V(q_2) = 771.3$ is still higher than $V(q_0)$, so that $q_0 \in \mathsf{Basin}(q_1)$. The equilibrium q_1 induced by $\|f_{ext}\| = 4$ N is depicted in Figure 6(d). The contact reaction forces in this case violate the friction cone constraints. For this preload level, the wrenches corresponding to force magnitudes up to $\|f_{ext}\| = 3.5$ N lie within $\overline{\mathcal{W}}_{ext}$.

Example 7: Next consider the same grasp with a higher preload level of ±5.8 N. For this preload level the initial grasp contains four equilibria—a stable equilibrium $q_1 = q_0$ depicted in Figure 7(a), another stable equilibrium q_2, and two unstable equilibria q_3 and q_4. For this preload level $V(q_0) = 580.0$. This value remains constant for all subsequent external forces. We apply external forces of magnitudes $\|f_{ext}\| = 1.5$, 3.0, and 4.5 N. The equilibrium q_1 induced by $\|f_{ext}\| = 1.5$ N is depicted in Figure 7(b). Note that $\mathcal{B}$ has significantly shifted

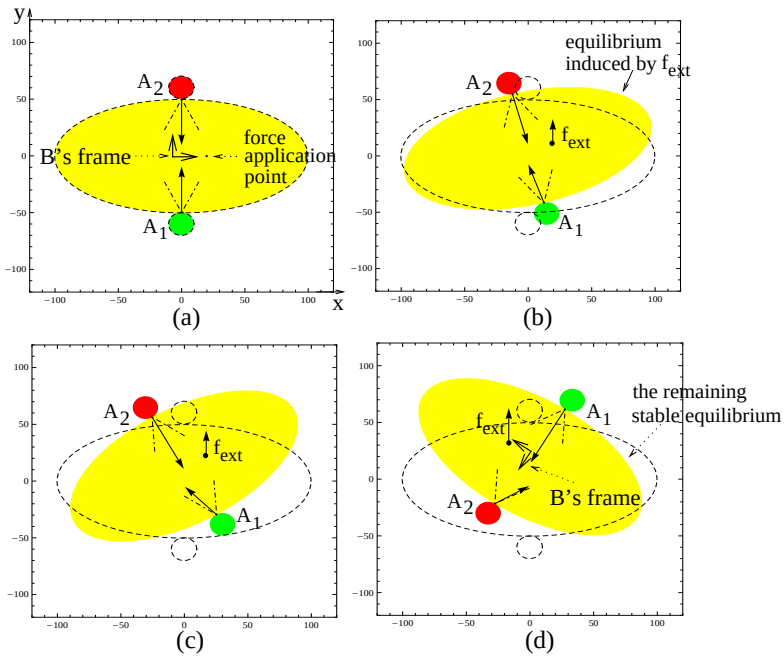

Figure 7: (a) The initial equilibrium grasp preloaded with ±5.8 N. (b)-(c) The stable equilibrium q_1 such that $q_0 \in \mathsf{Basin}(q_1)$ due to $\|f_{ext}\| = 1.5$ N and $\|f_{ext}\| = 3.0$ N. (d) The single stable equilibrium when $\|f_{ext}\| = 4.5$ N.

and rotated in response to this force, due to a higher grasp stiffness associated with this higher preload level. The contact reaction forces at q_1 lie within the friction cones. The value of V at the lower saddle is $V(q_3) = 597.6$. Since $V(q_0) < V(q_3)$, q_0 lies in $\mathsf{Basin}(q_1)$. The equilibrium q_1 induced by $\|f_{ext}\| = 3.0$ N is depicted in Figure 7(c). This equilibrium still satisfies the friction cone constraints. However, the set $\mathsf{Basin}(q_1)$ shrinks as discussed in Example 5, and now $V(q_3) = 553.2$. Since $V(q_0) > V(q_3)$, now q_0 lies outside $\mathsf{Basin}(q_1)$. For this preload level, the wrenches corresponding to force magnitudes up to $\|f_{ext}\| = 2.25$ N lie within $\overline{\mathcal{W}}_{ext}$. When $\|f_{ext}\|$ increases beyond 2.25 N, the equilibrium q_1 looses its local stability at $\|f_{ext}\| = 4.5$ N. At this value the number of equilibria decreases from four to two, and the ellipse starts to rotate toward the single stable equilibrium depicted in Figure 7(d). However, the ellipse will incur contact breakage during this motion.

4 Transient Behavior of the Passive Force Closure Set

Let q_1 be a stable equilibrium induced by $\boldsymbol{w}_{ext} \in \overline{\mathcal{W}}_{ext}$, so that $q_0 \in \mathsf{Basin}(q_1)$. This section describes a test ensuring that the fingertips do not break contact or slip during $\mathcal{B}$'s convergence from q_0 to q_1. Because the system is governed by a potential energy, the test is based on the following conservation of energy argument. Let $V(q)$ be $\mathcal{B}$'s total potential energy function under the influence of $\boldsymbol{w}_{ext}$. Let $V|_{\leq c}$ denote the sub-level set $V|_{\leq c} = \{q : V(q) \leq c\}$. Since $\mathcal{B}$ starts with zero velocity at q_0, its total mechanical energy is initially $V(q_0)$. Hence by conservation of energy $\mathcal{B}$'s entire trajectory lies in the set $V|_{\leq V(q_0)}$. Our objective is to ensure that the portion of $V|_{\leq V(q_0)}$ within $\mathsf{Basin}(q_1)$ would satisfy the friction cone constraints. We begin with a lemma which characterizes the sub-level sets of V.

Lemma 4.1. *Let $V(q)=\sum_{i=1}^{k}U_i(q)+U_g(q)+U_{ext}(q)$ be $\mathcal{B}$'s total potential energy function associated with the linear law (3), such that $\sum_{i=1}^{k}K_i>0$. Let q_1 be the stable equilibrium induced by $\boldsymbol{w}_{ext}\in\overline{\mathcal{W}}_{ext}$ such that $q_0\in\mathsf{Basin}(q_1)$. Then each sub-level set $V|_{\leq c}$ within $\mathsf{Basin}(q_1)$ is a topological solid ball whose fixed-θ slices form ellipses.*

Moreover, the fixed-θ ellipses are contained in discs whose radius is maximal at the θ-slice of q_1 and decreases monotonically to zero on both sides of q_1 (Figure 8).

Proof: Every sub-level set $V|_{\leq c}$ within $\mathsf{Basin}(q_1)$ is topologically equivalent to a solid ball (see proof of Lemma 3.5 in Appendix C). Moreover, when $\sum_{i=1}^{k}K_i>0$ the potential function $V(d,\theta)$ is quadratic positive definite in d (see proof of the same lemma). Hence each fixed-θ slice of $V|_{\leq c}$ forms an ellipse which can possibly degenerate to a single point.

Next we derive a formula for the discs containing the fixed-θ ellipses comprising $V|_{\leq c}$. Using the notation $P=\sum_{i=1}^{k}K_i$, each sub-level set of V can be written as the quadratic form: $V|_{\leq c}=\{q:\frac{1}{2}(d-\mathrm{v}(\theta))^TP(d-\mathrm{v}(\theta))\leq c+\nu(\theta)\}$, where

$$\mathrm{v}(\theta)=P^{-1}\big(f_{ext}-\sum_{i=1}^{k}K_i(\boldsymbol{\rho}_i(\theta)-y_i^0)\big) \tag{10}$$

and

$$\nu(\theta)=\tfrac{1}{2}\mathrm{v}(\theta)^TP\mathrm{v}(\theta)-\sum_{i=1}^{k}\big\{\tfrac{1}{2}\big(\boldsymbol{\rho}_i(\theta)-y_i^0\big)^TK_i\big(\boldsymbol{\rho}_i(\theta)-y_i^0\big)-f_i^0\cdot\boldsymbol{\rho}_i(\theta)\big\}-mg\boldsymbol{\rho}_c(\theta)\cdot\boldsymbol{e}+\boldsymbol{\rho}_{ext}(\theta)\cdot f_{ext}. \tag{11}$$

Let σ_{min} denote the minimal eigenvalue of P. Every $(d,\theta)\in V|_{\leq c}$ satisfies the inequality $\frac{1}{2}\sigma_{min}\|d-\mathrm{v}(\theta)\|^2\leq c+\nu(\theta)$. Since $V|_{\leq c}$ is topologically equivalent to a solid ball, it spans a θ interval containing the θ coordinate of q_1 in its interior. Let $[\theta_{min},\theta_{max}]$ denote this interval. Then the fixed-θ ellipses comprising $V|_{\leq c}$ are contained in discs with center at $\mathrm{v}(\theta)$ and radius $r(\theta)=\sqrt{2(c+\nu(\theta))/\sigma_{min}}$ for $\theta\in[\theta_{min},\theta_{max}]$.

We now establish that $r(\theta)$ decreases monotonically to zero on both sides of q_1's θ coordinate, denoted θ_1. The gradient of $V(d,\theta)=\frac{1}{2}(d-\mathrm{v}(\theta))^TP(d-\mathrm{v}(\theta))-\nu(\theta)$ is given by

$$\nabla V(d,\theta)=\begin{pmatrix}P(d-\mathrm{v}(\theta))\\ -\frac{1}{2}(d-\mathrm{v}(\theta))^TP\mathrm{v}'(\theta)-\nu'(\theta)\end{pmatrix}.$$

Consider now the points d^* satisfying $P(d^*-\mathrm{v}(\theta))=\vec{0}$ for $\theta\in[\theta_{min},\theta_{max}]$. The gradient of V at (d^*,θ) is: $\nabla V(d^*,\theta)=(\vec{0},-\nu'(\theta))$. Since q_1 is the only critical point of V in the interior of $\mathsf{Basin}(q_1)$, ∇V is non-vanishing in the portion of $V|_{\leq V(q_0)}$ within $\mathsf{Basin}(q_1)$, except at q_1. Hence $\nu'(\theta)\neq 0$ for $\theta\in(\theta_{min},\theta_{max})$ except at $\theta=\theta_1$. Since $r'(\theta)$ is a positive multiple of $\nu'(\theta)$, $r'(\theta)\neq 0$ for $\theta\in(\theta_{min},\theta_{max})$. Therefore $r(\theta)$ is strictly monotonic on both sides of θ_1. Since $r(\theta_1)>0$ while $r(\theta_{min})=r(\theta_{max})=0$, $r(\theta)$ is maximal at $\theta=\theta_1$ and decreases monotonically to zero at $\theta=\theta_{min}$ and θ_{max}. □

To ensure that the portion of $V|_{\leq V(q_0)}$ within $\mathsf{Basin}(q_1)$ satisfies the friction cone constraints, we first compute the θ interval spanned by this set. Based on the above proof, $V|_{\leq V(q_0)}=\{q:\frac{1}{2}(d-\mathrm{v}(\theta))^TP(d-\mathrm{v}(\theta))\leq V(q_0)+\nu(\theta)\}$, where $\mathrm{v}(\theta)$ and $\nu(\theta)$ are specified in (10) and (11). Hence $V|_{\leq V(q_0)}$ spans the θ interval satisfying $V(q_0)+\nu(\theta)\geq 0$. The term $V(q_0)+\nu(\theta)$ is a fourth-order polynomial in z under the identities $\sin(\theta)=2z/(1+z^2)$ and $\cos(\theta)=(1-z^2)/(1+z^2)$. The resulting polynomial is positive on either one or two intervals,

depending on the number of stable equilibria induced by $\boldsymbol{w}_{ext}$ (Lemma 3.3). The θ interval spanned by the portion of $V|_{\leq V(q_0)}$ within $\mathsf{Basin}(q_1)$, denoted $[\theta_{min}, \theta_{max}]$, is the interval containing θ_1 in its interior. Let r_V denote the maximal radius of the discs containing the fixed-θ ellipses of $V|_{\leq V(q_0)}$ for $[\theta_{min}, \theta_{max}]$ i.e., $\mathsf{r}_V = \sqrt{2(V(q_0)+\nu(\theta_1))/\sigma_{min}}$, where σ_{min} is the minimal eigenvalue of P. Based on this discussion, we define the *enclosing tube* of $V|_{\leq V(q_0)}$ as the set (see Figure 8):

$$\mathcal{T} = \{q : \|d - \mathrm{v}(\theta)\|^2 \leq \mathsf{r}_V^2\} \quad \theta \in [\theta_{min}, \theta_{max}].$$

The enclosing tube provides a conservative approximation for the sub-level set $V|_{\leq V(q_0)}$. It allows a closed-form test verifying the friction cone constraints along the entire transient trajectory. This test is discussed in the following proposition. In the proposition $\|K_i\|$ denotes the matrix norm: $\|K_i\| = \max_{\|u\|\leq 1}\{u^T K_i u\}$. Recall that $R(\theta)t_i$ and and $R(\theta)n_i$ are the unit tangent and inward unit normal to $\mathcal{B}$ at x_i.

Proposition 4.2 (Transient Response)**.** *Let $\boldsymbol{w}_{ext} \in \overline{\mathcal{W}}_{ext}$ induce a stable equilibrium q_1, so that $q_0 \in \mathsf{Basin}(q_1)$. Let $\mathcal{T}$ be the enclosing tube of the sub-level set $V|_{\leq V(q_0)}$ within $\mathsf{Basin}(q_1)$. The following inequality in θ guarantees that $f_i^n(q) > 0$ for all $q \in \mathcal{T}$,*

$$\big(-K_i(\mathrm{v}(\theta) + \boldsymbol{\rho}_i(\theta) - y_i^0) + f_i^0\big) \cdot R(\theta)n_i > \mathsf{r}_V\|K_i\| \qquad \theta \in [\theta_{min}, \theta_{max}], \tag{12}$$

while the following pair of inequalities in θ guarantees that $|f_i^t(q)| < \mu f_i^n(q)$ for all $q \in \mathcal{T}$,

$$\big(-K_i(\mathrm{v}(\theta) + \boldsymbol{\rho}_i(\theta) - y_i^0) + f_i^0\big) \cdot R(\theta)(\mu n_i \pm t_i) > \sqrt{1+\mu^2}\,\mathsf{r}_V\|K_i\| \quad \theta \in [\theta_{min}, \theta_{max}], \tag{13}$$

where r_V is the enclosing tube's radius and $[\theta_{min}, \theta_{max}]$ is the enclosing tube's θ interval.

The inequality (12) can be interpreted as follows. The left side of (12) is the value of f_i^n at the center $\mathrm{v}(\theta)$ of each fixed-θ slice of $\mathcal{T}$. The right side, $\mathsf{r}_V\|K_i\|$, is an upper bound on the variation in f_i^n due to c-space motion of $\mathcal{B}$ away from $\mathrm{v}(\theta)$ within this θ slice of $\mathcal{T}$. The inequality (12) thus ensures that f_i^n remains strictly positive within each fixed-θ slice of $\mathcal{T}$. An analogous interpretation holds for the two inequalities specified in (13).

Proof: First consider the normal load constraint, $f_i^n(q) > 0$. Substituting the linear law (3) in $f_i(q)$ gives: $f_i^n(q) = \big(-K_i\big(x_i(q) - y_i^0\big) + f_i^0\big) \cdot R(\theta)n_i$, where $x_i(q) = R(\theta)r_i + d$. Using the notation $\boldsymbol{\rho}_i(\theta) = R(\theta)r_i$ and treating θ as a parameter gives: $f_i^n(d) = \big(-K_i(d + \boldsymbol{\rho}_i(\theta) - y_i^0) + f_i^0\big) \cdot R(\theta)n_i$. Each fixed-$\theta$ slice of $\mathcal{T}$ is a disc satisfying the inequality $\|d - \mathrm{v}(\theta)\|^2 \leq \mathsf{r}_V^2$. The *minimal* value of $f_i^n(d)$ in each θ-slice of $\mathcal{T}$ occurs on the disc's boundary, at the point:

$$d^*(\theta) = \mathrm{v}(\theta) + \frac{\mathsf{r}_V}{\|K_i R(\theta)n_i\|} K_i R(\theta)n_i.$$

It follows that $\mathcal{T}$ satisfies the normal load constraint if $f_i^n(d^*(\theta), \theta) > 0$ for $\theta_{min} \leq \theta \leq \theta_{max}$. Substituting for $d^*(\theta)$ in $f_i^n(d)$ gives the inequality: $\big(-K_i(\mathrm{v}(\theta) + \boldsymbol{\rho}_i(\theta) - y_i^0) + f_i^0\big) \cdot R(\theta)n_i > \mathsf{r}_V\|K_i R(\theta)n_i\|$. Since $\|K_i R(\theta)n_i\| \leq \|K_i\|$, the stricter inequality specified in (12) guarantees that $f_i^n(q) > 0$ for all $q \in \mathcal{T}$.

Next consider the tangential load constraint, $|f_i^t(q)| < \mu f_i^n(q)$. This constraint is equivalent to the pair of inequalities: $f_i^t(q) < \mu f_i^n(q)$ and $-f_i^t(q) < \mu f_i^n(q)$. Substituting $f_i^t(q) = f_i(q) \cdot R(\theta)t_i$ and $f_i^n(q) = f_i(q) \cdot R(\theta)n_i$ gives the two inequalities: $f_i(q) \cdot R(\theta)(\mu n_i \pm t_i) > 0$.

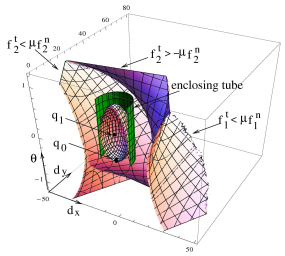

Figure 8: The enclosing tube of $V|_{\leq V(q_0)}$ and the friction cone constraints for a torque of $\tau_{ext} = 50$ N·mm acting on the ellipse of Example 2.

Substituting the linear law (3) in $f_i(q)$ gives: $\big(-K_i(d+\boldsymbol{\rho}_i(\theta)-y_i^0)+f_i^0\big)\cdot R(\theta)(\mu n_i \pm t_i) > 0$. The left-side expression attains a *minimal* value in each fixed-θ slice of $\mathcal{T}$ at the point:

$$d^*(\theta) = \mathrm{v}(\theta) + \frac{\mathsf{r}_V}{\|K_i R(\theta)(\mu n_i \pm t_i)\|} K_i R(\theta)(\mu n_i \pm t_i).$$

Therefore $\mathcal{T}$ satisfies the tangential load constraint if $|f_i^t(d^*(\theta),\theta)| \leq \mu f_i^n(d^*(\theta),\theta)$ for $\theta_{min} \leq \theta \leq \theta_{max}$. Substituting for $d^*(\theta)$ gives: $\big(-K_i(\mathrm{v}(\theta)+\boldsymbol{\rho}_i(\theta)-y_i^0)+f_i^0\big)\cdot R(\theta)(\mu n_i \pm t_i) > \mathsf{r}_V\|K_i R(\theta)(\mu n_i \pm t_i)\|$. Since $\|K_i R(\theta)(\mu n_i \pm t_i)\| \leq \sqrt{1+\mu^2}\|K_i\|$, the stricter inequalities specified in (13) guarantee that $|f_i^t(q)| < \mu f_i^n(q)$ for all $q \in \mathcal{T}$. □

The proposition provides a test ensuring that $\mathcal{B}$'s transient motion from q_0 to q_1 would not incur contact slippage or breakage. The procedure for checking that $\boldsymbol{w}_{ext} \in \overline{\mathcal{W}}_{ext}$ induces an admissible transient trajectory as follows. First compute the interval $[\theta_{min}, \theta_{max}]$ as discussed above. Since (12) and (13) are quadratic in $\sin(\theta)$ and $\cos(\theta)$, they become fourth-order polynomials in $z = \tan(\theta/2)$ under the identities $\sin(\theta) = 2z/(1+z^2)$ and $\cos(\theta) = (1-z^2)/(1+z^2)$. Each of these polynomials is strictly positive at $z = \tan(\theta_1/2)$, since by construction $q_1 = (d_1, \theta_1)$ satisfies the friction cone constraints. Hence each inequality is satisfied iff all its roots lie *outside* the interval $[\theta_{min}, \theta_{max}]$. By verifying (12) and (13) for all k contacts, one ensures that the entire trajectory of $\mathcal{B}$ from q_0 to q_1 satisfies the friction cone constraints.

Example 8: Consider the two-finger grasp of the ellipse discussed in Example 2. Let a disturbance torque $\tau_{ext} = 50$ N·mm act about the ellipse's center. Let q_1 be the stable equilibrium induced by τ_{ext} such that $q_0 \in \mathsf{Basin}(q_1)$. Figure 8 depicts the portion of the sub-

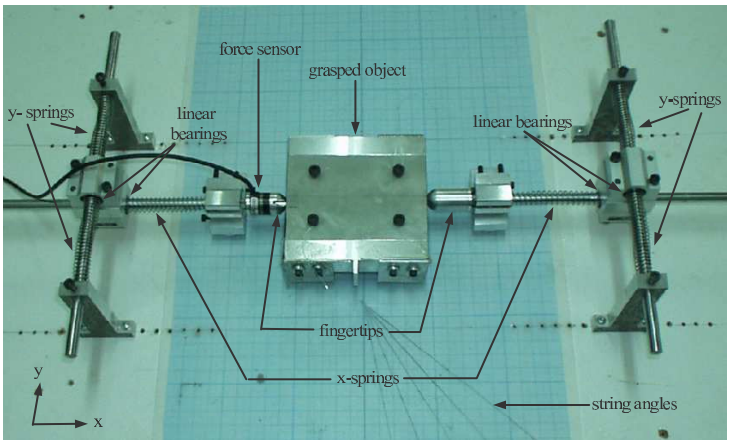

Figure 9: The two-finger grasping system used for the experiments.

level set $V|_{\leq V(q_0)}$ within $\mathsf{Basin}(q_1)$, as well as its enclosing tube $\mathcal{T}$. The figure also depicts the surfaces bounding the normal and tangential load constraint, $f_i^n(q) > 0$ and $|f_i^t(q)| \leq \mu f_i^n(q)$ for $i = 1, 2$. It can be seen that $\mathcal{T}$ satisfies the friction cone constraints, thus ensuring that the contacts do not break or slip during $\mathcal{B}$'s trajectory from q_0 to q_1.

5 Experimental Results

This section describes experiments conducted with the grasping system shown in Figure 9. The system lies in a horizontal plane and consists of two spring-loaded fingers. The fingers are initially preloaded against a freely moving rectangular object, then a series of external loads is applied until the fingers can no longer passively balance the current external load. The limit value is recorded and compared against the analytically computed boundary value of the passive force closure set. This process is then repeated for a new series of applied loads.

The details of the experimental apparatus are as follows. The fingertips are made of aluminum and have a spherical shape of radius 8.5 mm. These fingertips provide a reasonable approximation to our assumption of sharp-tipped fingers. Each fingertip is attached to a spring-loaded rod aligned with the x-axis. Each x-axis rod slides on linear bearings mounted within a connecting device (see Figure 9). The connecting device slides on linear bearings along an orthogonal spring-loaded rod aligned with the y-axis. Each y-axis rod is clamped at its endpoints to the supporting table. The resulting spring loaded fingers obey a linear contact law with a diagonal contact stiffness matrix, $K_i = \begin{bmatrix} \kappa_x & 0 \\ 0 & \kappa_y \end{bmatrix}$ for $i = 1, 2$.[5] Using an ATI Nano 17 force sensor, the spring stiffnesses were determined to be $\kappa_x = 0.11$ and $\kappa_y = 0.14$ N/mm. The object is a flat aluminum block having dimensions 100×100×20 mm. It is passively supported by roller balls mounted inside a rectangular frame attached to the supporting table. Similar roller balls support the base of the two fingertips. The dominant frictional forces influencing the grasped object are generated at the fingertips. As a preliminary step, the friction coefficient at the fingertips was determined to be $\mu = 0.5$, with a standard deviation of $\pm 6.5\%$.

[5]This topic is further discussed in Ref. [32]—the springs apply linear forces on the sliding rods, which in turn induce linear force-displacement laws at the fingertips.

The experiments began with a preloading of the fingers along the x-axis by opposing forces of magnitude 5.8 N. Each experiment involved the application of a force along a fixed direction having a successively increasing magnitude. The forces were applied via a string attached to the object and pulled by weights which were incremented by 50 gram. This process was repeated for six string angles $0°, 10°, 20°, 30°, 40°, 50°$, measured with respect to the downward y-axis. The string's attachment point and directions are marked on the supporting table in Figure 9. Since the string is attached at the object's perimeter, all non-zero string directions generate non-zero torques about the object's center, with a higher torque as the string's angle increases from 0° to 50°. Due to the limited physical space within the experimental setup, we were not able to increase the loading angle beyond 50°.

Recall now that a candidate $\boldsymbol{w}_{ext}$ lies in the passive force closure set if it can be balanced at an equilibrium $q_1 \in \mathcal{FQ} \cap \mathcal{FP}$ such that $q_0 \in \mathsf{Basin}(q_1)$. However, the experiments involve a *gradual* increase of the external load, with a settling of the spring-loaded fingers at a new equilibrium after each force application. Each new equilibrium thus forms the initial equilibrium for the next one associated with a higher force magnitude. Since the force magnitudes increase by modest 50 gram increments, we experimentally observed that each equilibrium automatically lies in the basin of attraction of the next equilibrium. The experiments therefore only verify that $\mathcal{FQ} \cap \mathcal{FP}$ delineates the passive force closure set under gradual, or quasi-static, increase of the external load.

The experiments are summarized in Figure 10. Each dot and cross represents an external wrench applied during one measurement. The measurements are arranged along six rays emanating from the object's wrench space origin. The solid dots indicate external loads that were stably balanced by the fingers without any contact breakage or slippage. The cross indicates an external load which incurred contact slippage, while the circled crosses indicate external loads which incurred contact breakage followed by a gross motion of the object. Note that the fixed force-magnitude increments result in equal spacing of the measurements along each ray. However, the amount of spacing increases with the applied load angle, due to an increasing torque component at larger string angles. Figure 10 also depicts the analytically computed facets of the set $\mathcal{W}_{ext}$, delineating the local conditions for the passive closure set. While the measurements form a fairly coarse sampling of wrench space, all dot-to-cross transitions match the analytically computed boundary of $\mathcal{W}_{ext}$. Moreover, contact slippage occured only along the zero-degree ray, while contact breakage followed by a gross motion occured along all other rays. This is consistent with the fact that the zero degree ray crosses the side-facet of $\mathcal{W}_{ext}$ which corresponds to contact slippage, while all other rays cross the top facet of $\mathcal{W}_{ext}$ which correspond to loss of stability. The experiments thus corroborate the local conditions for the passive force closure set.

6 Conclusion

This paper considered grasps and fixtures whose contacts react according to force displacement laws consistent with friction constrains at the contacts. The passive force closure set of such grasps and fixtures is the collection of external wrenches that can be stably balanced by the reactive contacts. An external wrench $\boldsymbol{w}_{ext}$ belongs to the passive force closure set if it satisfies two types of constraints. First, $\boldsymbol{w}_{ext}$ must induce an equilibrium q_1 which is locally stable and satisfies the friction cone constraints. Second, the basin of attraction of q_1,

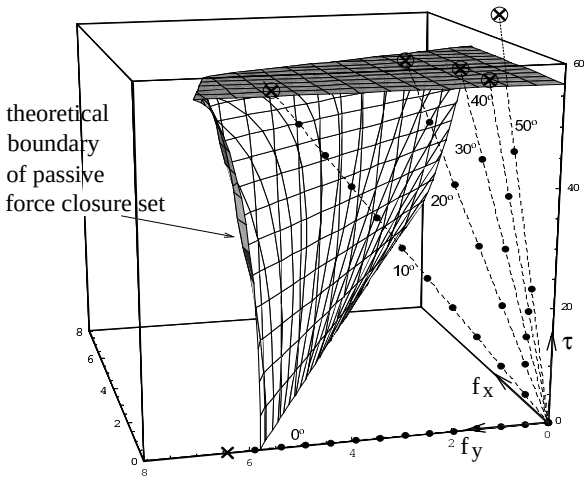

Figure 10: The applied external loads which induce stable equilibria (solid dots), contact slippage (a cross), and unstable motion involving contact breakage (circled crosses).

$\mathsf{Basin}(q_1)$, must include the initial unperturbed equilibrium configuration q_0. The paper subsequently focused on *linear* force-displacement laws. Under this setting no matter how many contacts participate in the grasp, every $\boldsymbol{w}_{ext}$ induces either two or four equilibria. In the first case one equilibrium is a minimum while the other is a saddle of the grasp's total potential energy function. In the second case two equilibria are minima while the other two are saddles of the grasp's total potential energy function. In the first case $\mathsf{Basin}(q_1)$ is bounded by the topological sphere formed by the level surface passing through the saddle. In the second case $\mathsf{Basin}(q_1)$ is bounded by the topological sphere formed by the level surface passing through the lower saddle, such that the sphere lies between the fixed-θ planes passing through the two saddles and containing the initial equilibrium q_0. This characterization lead to a closed form expression for the requirement $q_0 \in \mathsf{Basin}(q_1)$. The paper also provided a conservative test ensuring that $\mathcal{B}$'s transient trajectory from q_0 to the equilibrium induced by $\boldsymbol{w}_{ext}$ would not incur contact slippage or breakage. Finally, experiments with a spring-loaded grasping system corroborated the local conditions for the passive force closure set.

Let us discuss some extensions and future research topics. A fundamental question that needs further investigation is under what conditions the grasped object has two or four equilibrium configurations. Understanding the physical meaning of these conditions may guide our development of grasp synthesis tools. We are currently developing such synthesis tools based on the passive force closure set. The two most important synthesis parameters are the contact locations and preload forces. Both of these parameters appear explicitly in the passive closure set expressions. Our current work strives to obtain a procedure for contact and preload selection such that a given neighborhood of disturbance wrenches will be contained in the grasp's passive force closure set. Since the passive force closure set is non-convex and is affected in a non-trivial manner by the above parameters, this is a challenging objective. Another research challenge is to extend the passive force closure set to planar grasps and fixtures whose fingertips are not necessarily sharp tipped. Our preliminary research indicates that in this case too, each external wrench induces a finite number of equilibria [30][p. 39-49]. Since the fingertips can now roll along the object's boundary in response to an applied wrench, local stability of the induced equilibria now depends on the first as well as second-order geometry of the contacting bodies [19, 23, 36]. The

characterization of the passive force closure set in this more general setting is a challenging open problem currently under investigation.

Finally, recall our comment on the applicability of the results to quasistatic locomotion synthesis. For instance, our three-legged robot moves in planar tunnel environments by bracing itself against the environment with two limbs while lifting its free limb to a new position [26]. By synthesizing the limb's lifting phases based on the passive force closure set, one can guarantee that disturbance wrenches generated by the moving limb will be stably balanced by the bracing contacts. Finally, our longer term goal is to extend the notion of the passive closure set to three-dimensions, making it useful for quasistatic locomotion over three-dimensional terrains.

A Details of the Passive Force Closure Criterion

This appendix contains a proof sketch of the passive force closure criterion. In the following proposition $U(q) = \sum_{i=1}^{k} U_i(q) + U_g(q)$.

Proposition 2.1. *Let $\mathcal{B}$ be held at an equilibrium grasp by k contacts satisfying the linear force-displacement law (2). Let $U(q)$ be $\mathcal{B}$'s total potential energy. If the grasp is non-marginal and forms a non-degenerate local minimum of U, it is* **passive force closure.**

Proof sketch: Let q_0 be $\mathcal{B}$'s initial equilibrium grasp configuration. Let a fixed collection of forces act at various points of $\mathcal{B}$ and generate a net wrench $\boldsymbol{w}_{ext}$. We have to show that any sufficiently small $\boldsymbol{w}_{ext}$ can be balanced by the contacts at a nearby equilibrium, denoted q_1, such that q_0 lies in the basin of attraction of q_1. We first show that all sufficiently small $\boldsymbol{w}_{ext}$ can be balanced by the contacts. Since the fingertips are preloaded against $\mathcal{B}$ at q_0, local motions of $\mathcal{B}$ about q_0 do not incur any contact breakage. Since q_0 is a non-marginal equilibrium grasp, the contact reaction forces induced by local motions of $\mathcal{B}$ remain in their friction-cones' interior. Hence there exists a c-space neighborhood about q_0, denoted $\mathcal{N}$, such that $\mathcal{B}$ retains its k contacts without breakage or slippage for all $q \in \mathcal{N}$.

The net wrench generated on $\mathcal{B}$ by the k contacts and gravity is given by $-\nabla U(q)$. Hence an equilibrium configuration induced by $\boldsymbol{w}_{ext}$ satisfies $-\nabla U(q) + \boldsymbol{w}_{ext} = \vec{0}$. We now show that the set of wrenches $\mathcal{W} = \{\nabla U(q) : q \in \mathcal{N}\}$ contains an open neighborhood about the origin in wrench space. Consider $\nabla U(q)$ as a mapping from c-space to wrench space,[6] $\nabla U(q) : I\!R^3 \rightarrow I\!R^3$. By assumption $\nabla U(q_0) = \vec{0}$. According to the Inverse Function Theorem, a non-singular derivative of ∇U at q_0, $D^2U(q_0)$, guarantees that ∇U maps an open neighborhood about q_0 onto an open neighborhood about the origin in wrench space. Since q_0 is a non-degenerate local minimum of U, $D^2U(q_0)$ is non-singular. Therefore, by shrinking $\mathcal{N}$ if necessary, $\mathcal{W}$ forms an open neighborhood about the wrench space origin such that every $\boldsymbol{w}_{ext} \in \mathcal{W}$ induces an equilibrium at some configuration $q \in \mathcal{N}$.

Let us now establish that by further shrinking $\mathcal{W}$, every $\boldsymbol{w}_{ext} \in \mathcal{W}$ induces a locally stable equilibrium. Consider for simplicity the case where $\boldsymbol{w}_{ext}$ is generated by a single fixed force, f_{ext}, acting on $\mathcal{B}$ at the point $x_{ext} = R(\theta)r_{ext} + d$. Then $\boldsymbol{w}_{ext}$ is the negated gradient of the potential function $U_{ext}(q) = -x_{ext}(q) \cdot f_{ext}$. Based on this observation, the dynamics

[6] Technically, $\nabla U(q)$ maps a neighborhood about $q_0 \in I\!R^3$ to a neighborhood about $(q_0, 0)$ in the cotangent bundle $T^*I\!R^3$, which is then projected to a neighborhood about the origin in wrench space $T^*_{q_0}I\!R^3$.

of $\mathcal{B}$ is given by

$$M(q)\ddot{q} + C(q,\dot{q}) = -\nabla V(q) \qquad \text{where } V(q) = U(q) + U_{ext}(q),$$

where $M(q)$ is $\mathcal{B}$'s inertia matrix and $C(q,\dot{q})$ are Coriolis and centrifugal forces acting on $\mathcal{B}$. The contacts also apply natural damping forces which we ignore for simplicity. (These damping forces arise from viscoelastic rolling phenomena associated with material compression at the contacts. See [14, p. 302-308] as well as [6].) In general, the flow of a damped mechanical system governed by a potential function is attracted to the local minima of this function [15]. It follows that any equilibrium $q \in \mathcal{N}$ is locally stable if it is a local minimum of V i.e., if $D^2V(q) > 0$.

We now verify that by suitably shrinking the set $\mathcal{N}$, $D^2V(q) = D^2U(q) + D^2U_{ext}(q) > 0$ for all $q \in \mathcal{N}$. The eigenvalues of D^2U vary continuously with q. Since $D^2U(q_0) > 0$, D^2U is positive definite in a neighborhood of q_0. Let $\mathcal{D}$ be a compact ball centered at q_0 and contained in the set $\{q \in I\!R^3 : D^2U(q) > 0\}$. Since $\mathcal{D}$ is compact, the minimal eigenvalue of D^2U in $\mathcal{D}$ is lower bounded by a constant $\lambda_0 > 0$. The summand D^2U_{ext} is given by $D^2U_{ext}(q) = \begin{bmatrix} 0 & 0 \\ 0 & \boldsymbol{\rho}_{ext}(\theta) \cdot f_{ext} \end{bmatrix}$, where $\boldsymbol{\rho}_{ext}(\theta) = R(\theta) r_{ext}$. Hence $\lambda_{min}(D^2V(q)) \geq \lambda_0 - |\boldsymbol{\rho}_{ext}(\theta) \cdot f_{ext}|$ in $\mathcal{D}$. It follows that the inequality $|\boldsymbol{\rho}_{ext}(\theta) \cdot f_{ext}| < \lambda_0$ guarantees that $D^2V > 0$ in $\mathcal{D}$. Observe now that $\boldsymbol{w}_{ext} = (f_{ext}, \boldsymbol{\rho}_{ext}(\theta) \times f_{ext})$ satisfies the inequality $\|\boldsymbol{w}_{ext}\| \geq \|f_{ext}\|$. Let $\mathcal{W}_{\mathcal{D}}$ be the open neighborhood about the wrench space origin defined by $\mathcal{W}_{\mathcal{D}} = \{\boldsymbol{w} : \|\boldsymbol{w}\| < \lambda_0 / \|r_{ext}\|\}$. Since $\|\boldsymbol{w}_{ext}\| \geq \|f_{ext}\|$, the wrenches $\boldsymbol{w}_{ext} \in \mathcal{W}_{\mathcal{D}}$ are generated by forces satisfying $\|f_{ext}\| < \lambda_0 / \|r_{ext}\|$. Hence $|\boldsymbol{\rho}_{ext}(\theta) \cdot f_{ext}| \leq \|r_{ext}\| \|f_{ext}\| < \lambda_0$ for all $\boldsymbol{w}_{ext} \in \mathcal{W}_{\mathcal{D}}$. By shrinking $\mathcal{N}$ and $\mathcal{W}$ such that $\mathcal{N} \subseteq \mathcal{D}$ and $\mathcal{W} \subseteq \mathcal{W}_{\mathcal{D}}$, every $\boldsymbol{w}_{ext} \in \mathcal{W}$ is balanced at a locally stable equilibrium configuration $q \in \mathcal{N}$. Note that $\mathcal{N}$ still contains the initial equilibrium q_0, while $\mathcal{W}$ still forms an open neighborhood about the wrench space origin.

Let $q_1 \in \mathcal{N}$ be the locally stable equilibrium induced by $\boldsymbol{w}_{ext} \in \mathcal{W}$. Then q_1 is a local minimum of $V(q) = U(q) + U_{ext}(q)$. Our final task is to establish that $\mathcal{B}$ converges from its initial configuration at q_0 to the equilibrium q_1 induced by $\boldsymbol{w}_{ext} \in \mathcal{W}$. Since $D^2V(q) > 0$ for all $q \in \mathcal{D}$, the potential function V is strictly convex on $\mathcal{D}$. Hence any local minimum of V in $\mathcal{D}$ is its *global* minimum in this set. Since $q_1 \in \mathcal{N}$ and $\mathcal{N} \subseteq \mathcal{D}$, q_1 must be the global minimum of V in $\mathcal{D}$. In particular $q_0 \in \mathcal{D}$ lies in the basin of attraction of q_1 under the gradient flow $\dot{q} = -\nabla V(q)$. Since $\mathcal{B}$ starts with zero velocity at q_0, its total mechanical energy is initially $V(q_0)$. Hence by conservation of energy $\mathcal{B}$'s trajectory must converge to q_1. It follows that every $\boldsymbol{w}_{ext} \in \mathcal{W}$ induces an equilibrium $q_1 \in \mathcal{N}$ whose basin of attraction includes the initial equilibrium q_0. □

B Computation of the Grasp Stiffness Matrix

This appendix derives formulas for $D^2U_i(q), D^2U_g(q), D^2U_{ext}(q)$ which appear in the Hessian of $V(q) = \sum_{i=1}^{k} U_i(q) + U_g(q) + U_{ext}(q)$, then it provides a proof of Lemma 3.1. The elastic energy induced by the i^{th} linear contact law (3) is

$$U_i(q) = \tfrac{1}{2}(x_i(q) - y_i^0)^T K_i (x_i(q) - y_i^0) - f_i^0 \cdot x_i(q),$$

where $x_i(q) = R(\theta) r_i + d$ for $i = 1 \ldots k$. Since we assume that $\mathcal{B}$ is held at a non-marginal grasp, the fingertips can only roll at the contacts in response to local motions of $\mathcal{B}$. Under

our assumption that $\mathcal{B}$ is held by sharp-tipped fingers, the rolling tips maintain fixed contacts on $\mathcal{B}$'s boundary. Hence $r_i = r_i^0$, where r_i^0 is the fixed i^{th} tip position in $\mathcal{B}$'s reference frame. In the following, $X_{r_i}(q) = R(\theta)r_i^0 + d$ for $i = 1 \ldots k$.

The gradient of U_i is: $\nabla U_i(q) = -DX_{r_i}^T(q) f_i(q)$, where $f_i(q) = -K_i(X_{r_i}(q) - y_i^0) + f_i^0$. It follows that the second derivative of U_i is

$$D^2U_i(q) = DX_{r_i}^T(q) K_i DX_{r_i}(q) - D^2X_{r_i}^T(q) f_i(q). \tag{14}$$

The Jacobian $DX_{r_i}(q)$ is the 2×3 matrix $DX_{r_i}(q) = [I\ J\boldsymbol{\rho}_i]$, where I is the 2×2 identity matrix, $J = \left[\begin{smallmatrix} 0 & 1 \\ -1 & 0 \end{smallmatrix}\right]$, and $\boldsymbol{\rho}_i = R(\theta)r_i^0$. The second derivative, $D^2X_{r_i}(q)$, is a vector-valued symmetric bilinear function. To obtain a formula for $D^2X_{r_i}(q)$, we compute the derivative of $DX_{r_i}(q)$ along a c-space trajectory $q(t)$. Recall that $\mathcal{B}$'s velocity along $q(t)$ is denoted $\dot{q} = (v, \omega)$, where $\omega \in I\!R$ is $\mathcal{B}$'s angular velocity. Thus $\frac{d}{dt}DX_{r_i}(q(t)) = \big[0\ J\dot{R}r_i^0\big] = \big[0\ -\boldsymbol{\rho}_i\omega\big]$, where we used the identity $J^2 = -I$. The action of this derivative on f_i is: $\big(\frac{d}{dt}DX_{r_i}^T(q(t))\big)f_i = \begin{pmatrix} 0 \\ (-\boldsymbol{\rho}_i \cdot f_i)\omega \end{pmatrix}$. On the other hand, $\frac{d}{dt}DX_{r_i}(q(t)) = (D^2X_{r_i}(q))\dot{q}$ by the chain rule. Hence the action of $D^2X_{r_i}(q)^T$ on f_i is the 3×3 matrix:

$$D^2X_{r_i}(q)^T f_i = \begin{bmatrix} O & 0 \\ 0^T & -\boldsymbol{\rho}_i \cdot f_i \end{bmatrix},$$

where O is a 2×2 matrix of zeroes. Substituting for $DX_{r_i}(q)$ and $D^2X_{r_i}(q)^T f_i$ in (14) gives

$$D^2U_i(q) = [I\ J\boldsymbol{\rho}_i]^T K_i [I\ J\boldsymbol{\rho}_i] + \begin{bmatrix} O & 0 \\ 0^T & \boldsymbol{\rho}_i \cdot f_i \end{bmatrix},$$

where O is a 2×2 matrix of zeroes. Next we consider the formula for D^2U_g. The gravitational potential energy is given by $U_g(q) = mg\,\boldsymbol{e} \cdot x_c(q)$, where $x_c(q) = R(\theta)r_c + d$. Since r_c is fixed in $\mathcal{B}$'s reference frame, the formulas for $Dx_c(q)$ and $D^2x_c(q)$ are similar to the formulas for $DX_{r_i}(q)$ and $D^2X_{r_i}(q)$. Based on these formulas,

$$D^2U_g(q) = mg \begin{bmatrix} O & 0 \\ 0^T & -\boldsymbol{\rho}_c \cdot \boldsymbol{e} \end{bmatrix} \quad \text{where } \boldsymbol{\rho}_c = R(\theta)r_c.$$

Finally, $U_{ext}(q) = -f_{ext} \cdot x_{ext}(q)$ where $x_{ext}(q) = R(\theta)r_{ext} + d$. Since f_{ext} is a fixed force and r_{ext} is a fixed point in $\mathcal{B}$'s reference frame, the formula for D^2U_{ext} is:

$$D^2U_{ext} = \begin{bmatrix} O & 0 \\ 0^T & \boldsymbol{\rho}_{ext} \cdot f_{ext} \end{bmatrix} \quad \text{where } \boldsymbol{\rho}_{ext} = R(\theta)r_{ext}.$$

The following lemma provides an expression for the local stability set $\mathcal{PQ}$.

Lemma 3.1. *Let a planar object $\mathcal{B}$ be held by k contacts satisfying the linear force-displacement law (3), such that $\sum_{i=1}^k K_i > 0$. The set of $\mathcal{B}$'s locally stable equilibrium configurations, $\mathcal{PQ} = \{q : \lambda_{min}\big(D^2V(q)\big) > 0\}$, is given by*

$$\mathcal{PQ} = \Big\{q : P_{22} - P_{12}^T P_{11}^{-1} P_{12} + \sum_{i=1}^{k} f_i(q) \cdot (\boldsymbol{\rho}_i - \boldsymbol{\rho}_{ext}) + (\boldsymbol{\rho}_c - \boldsymbol{\rho}_{ext}) \cdot f_g > 0\Big\},$$

where $P_{11} = \sum_{i=1}^k K_i$, $P_{12} = \sum_{i=1}^k K_i J\boldsymbol{\rho}_i$, $P_{22} = \sum_{i=1}^k (J\boldsymbol{\rho}_i)^T K_i J\boldsymbol{\rho}_i$ ($\boldsymbol{\rho}_i, \boldsymbol{\rho}_c, \boldsymbol{\rho}_{ext}$ depend on θ).

Proof: Let us first express the Hessian of V in terms of P_{11}, P_{12}, and P_{22}:

$$D^2V(q) = \begin{bmatrix} P_{11} & P_{12} \\ P_{12}^T & P_{22} \end{bmatrix} + \begin{bmatrix} O & 0 \\ 0^T & \sum_{i=1}^k f_i(q)\cdot\boldsymbol{\rho}_i + \boldsymbol{\rho}_c\cdot f_g + \boldsymbol{\rho}_{ext}\cdot f_{ext} \end{bmatrix}.$$

Consider now the transformation of the first summand:[7]

$$\begin{bmatrix} I & -P_{11}^{-1}P_{12} \\ 0 & 1 \end{bmatrix}^T \begin{bmatrix} P_{11} & P_{12} \\ P_{12}^T & P_{22} \end{bmatrix} \begin{bmatrix} I & -P_{11}^{-1}P_{12} \\ 0 & 1 \end{bmatrix} = \begin{bmatrix} P_{11} & 0 \\ 0^T & P_{22} - P_{12}^T P_{11}^{-1} P_{12} \end{bmatrix}.$$

Since the second summand of D^2V is invariant under this transformation, D^2V is related by the transformation to the block-diagonal matrix:

$$D^2V(q) \sim \begin{bmatrix} P_{11} & 0 \\ 0^T & P_{22} - P_{12}^T P_{11}^{-1} P_{12} + \sum_{i=1}^k f_i(q)\cdot\boldsymbol{\rho}_i + \boldsymbol{\rho}_c\cdot f_g + \boldsymbol{\rho}_{ext}\cdot f_{ext} \end{bmatrix}. \tag{15}$$

When A and P are $n \times n$ matrices such that A is non-singular and P symmetric, the eigenvalues of A^TPA have the same sign as the eigenvalues of P. Based on this fact, the condition $\lambda_{min}\big(D^2V(q)\big) > 0$ is equivalent to positiveness definiteness of the block diagonal matrix in (15). Since $P_{11} = \sum_{i=1}^k K_i > 0$, the latter matrix is positive definite iff its lower-right term is strictly positive. Since q is an equilibrium configuration, $f_{ext} = -(\sum_{i=1}^k f_i(q) + f_g)$. Substituting for f_{ext} in the lower-right term of (15) gives the result. □

C Stability Classification of Equilibrium Points

This appendix classifies the stability of the critical points of $\mathcal{B}$'s potential function $V(q) = \sum_{i=1}^k U_i(q) + U_g(q) + U_{ext}(q)$. The classification is based on Morse Theory [9, 17], whose relevant results are now reviewed. Recall that a set is compact if it is closed and bounded. Let $\mathcal{M}$ be a smooth and compact n-dimensional manifold,[8] and let $h : \mathcal{M} \to I\!R$ be a smooth real-valued function on $\mathcal{M}$. A point $p \in \mathcal{M}$ is a *critical* point of h if its derivative, $Dh(p)$, vanishes at this point. A *critical value* of h is the image $c = h(p)$ of a critical point p. Morse Theory requires that h be a Morse function. A function h is a *Morse* if all its critical points are non-degenerate i.e., if $D^2h(p)$ has full rank at the critical points. In general, almost all smooth functions are Morse functions. The *Morse index* of h at a critical point p, denoted λ, is the number of negative eigenvalues of the matrix $D^2h(p)$. Since $\mathcal{M}$ is an n-dimensional manifold, $0 \le \lambda \le n$. At a local minimum $\lambda = 0$ since all eigenvalues are positive, at the saddles $0 < \lambda < n$, while at a local maximum $\lambda = n$ since all eigenvalues are negative.

The two main results of Morse Theory are as follows. The first result asserts that as the value of h varies between two adjacent critical values, the level-sets $\mathcal{M}|_c = \{x \in \mathcal{M} : h(x) = c\}$ are *topologically equivalent* (homeomorphic) to each other, and the topological type of the sub-level sets $\mathcal{M}|_{\le c} = \{x \in \mathcal{M} : h(x) \le c\}$ remains constant. Any topological change in the level-sets must occur locally at the critical points of h. In particular, the path-connectivity of $\mathcal{M}|_c$ is preserved between critical values of h. Let p_0 be a critical point of h, with $c_0 = h(p_0)$. The second result characterizes the topological change in the level-sets

[7] The transformation is induced by a translation of $\mathcal{B}$'s reference frame to the grasp's center of compliance.

[8] Recall that an n-dimensional manifold is a hypersurface that locally looks like $I\!R^n$ at each of its points.

as c passes through a critical value c_0. Let D^i denote the unit i-dimensional ball and let S^{i-1} denote its boundary, the unit $(i-1)$-dimensional sphere. In particular, D^1 is a unit interval and S^0 consists of its two endpoints, while D^0 is an isolated point and its boundary is the empty set. Then the set $\mathcal{M}|_{\leq c_0+\epsilon}$ is obtained by "gluing" to the set $\mathcal{M}|_{\leq c_0-\epsilon}$ a "handle" of the form $\mathcal{H} = D^\lambda \times D^{n-\lambda}$, along a "gluing seam" $\mathcal{G} = S^{\lambda-1} \times D^{n-\lambda}$, where $\mathcal{G} \subset \mathcal{M}|_{c_0-\epsilon}$ and ϵ is an arbitrarily small constant. The pair $(\mathcal{H}, \mathcal{G})$ is called the *Morse data* at p_0.

Critical point	Morse data $(\mathcal{H}, \mathcal{G})$
A local minimum	$(D^0 \times D^3, \emptyset \times D^3) =$ 
A saddle with one negative eigenvalue	$(D^1 \times D^2, S^0 \times D^2) =$ 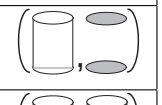
A saddle with two negative eigenvalues	$(D^2 \times D^1, S^1 \times D^1) =$ 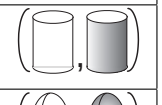
A local maximum	$(D^3 \times D^0, S^2 \times D^0) =$ 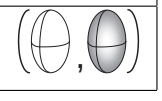

Table 1: The Morse data at the critical points of V on $\mathbb{R}^2 \times S^1$.

We now characterize the level sets of V using Morse Theory. Since $\mathcal{B}$'s θ coordinate is periodic in 2π, $\mathcal{B}$'s c-space is topologically equivalent to the three-dimensional manifold $\mathbb{R}^2 \times S^1$. However, $\mathbb{R}^2 \times S^1$ is not compact as required under Morse Theory. Hence we first embed this space in the compact manifold $S^2 \times S^1$, where S^2 is the unit sphere. This embedding entails an embedding of $\mathbb{R}^2$ in S^2 by identifying the points "at infinity" in $\mathbb{R}^2$ with the "north pole" in S^2. It can be verified that the function induced from V by this embedding is smooth on the entire manifold $S^2 \times S^1$ [18][p. 8-9]. Thus we may apply Morse theory directly to V on $\mathbb{R}^2 \times S^1$, with the understanding that $\mathbb{R}^2 \times S^1$ is embedded in the compact manifold $S^2 \times S^1$. The Morse data at the possible critical points of V is summarized in Table 1.

Lemma 3.4. *Let a planar object $\mathcal{B}$ be grasped by k contacts satisfying the linear contact law (3), such that $\sum_{i=1}^k K_i > 0$. When $\boldsymbol{w}_{ext} \in \mathcal{W}_{ext}$ induces two equilibria, one is locally stable while the other is an unstable saddle. When $\boldsymbol{w}_{ext} \in \mathcal{W}_{ext}$ induces four equilibria, two are locally stable while the other two are unstable saddles.*

Proof: Recall that $\mathcal{B}$'s potential function under the influence of $\boldsymbol{w}_{ext}$ is given by $V(q) = \sum_{i=1}^k U_i(q) + U_g(q) - \boldsymbol{w}_{ext} \cdot q$. The locally stable equilibria of $\mathcal{B}$ are the local minima of the potential function V, while the unstable equilibria are either saddles or local maxima of this function. We first establish that V can only have local minima or saddles with Morse index $\lambda = 1$. The second derivative matrix of V is given by $D^2V(q) = \sum_{i=1}^k D^2U_i(q) + D^2U_g(q)$. According to Appendix B, the formulas for $D^2U_i(q)$ and $D^2U_g(q)$ are given by

$$D^2U_i(q) = [I \; J\boldsymbol{\rho}_i]^T \, K_i \, [I \; J\boldsymbol{\rho}_i] + \begin{bmatrix} O & 0 \\ 0^T & \boldsymbol{\rho}_i \cdot f_i \end{bmatrix}$$

and

$$D^2U_g(q) = -mg \begin{bmatrix} O & 0 \\ 0^T & \boldsymbol{\rho}_c \cdot \boldsymbol{e} \end{bmatrix},$$

where $[I\ J\boldsymbol{\rho}_i]$ is a 2×3 matrix such that I is a 2×2 identity matrix and $J=\left[\begin{smallmatrix} 0 & 1 \\ -1 & 0 \end{smallmatrix}\right]$. Substituting for $D^2U_i(q)$ and $D^2U_g(q)$ in $D^2V(q)$, then evaluating $\dot{q}^T D^2V(q)\dot{q}$ along instantaneous translations of $\mathcal{B}$ represented by $\dot{q}=(v,0)$, gives $\dot{q}^T D^2V(q)\dot{q} = v^T\big(\sum_{i=1}^k K_i\big)v$. Since by assumption $\sum_{i=1}^k K_i > 0$, $D^2V(q)$ has at least two positive eigenvalues at any q. In particular, the Morse index at the critical points of V can be either $\lambda=0$ or $\lambda=1$.

Consider now the case where $\boldsymbol{w}_{ext}$ induces two equilibria, q_1 and q_2. Since $\boldsymbol{w}_{ext}\in\mathcal{W}_{ext}$, one of the two equilibria, say q_1, satisfies $\boldsymbol{w}_{ext}+\boldsymbol{w}(q_1)=\vec{0}$ such that $q_1\in\mathcal{F}Q\cap\mathcal{P}Q$. Since $D^2U(q)>0$ on $\mathcal{P}Q$ and $D^2V=D^2U$, the equilibrium at q_1 is a local minimum of V. We now show that q_2 must be a saddle of V. Suppose to the contrary, that q_2 is a local minimum of V. Let $c_1=V(q_1)$ and $c_2=V(q_2)$ be the two critical values of V, where we may assume that $c_1\le c_2$. According to Morse theory the topological type of the sub-level sets changes only when the value of V crosses c_1 and c_2. The Morse data at q_1 consist of $\mathcal{H}=D^3$ which is glued to $\mathcal{G}=\emptyset$ at q_1 (Table 1). Hence the sub-level sets $V_{\le c}$ such that $c_1<c<c_2$ are topologically equivalent to the solid ball D^3. When the value of V crosses c_2, a new *isolated* ball appears at the local minimum q_2. Hence the sub-level set $V_{\le c_2+\epsilon}$ is topologically equivalent to two disjoint solid balls. Since V has no other critical values beyond c_2, the sub-level set $V_{\le c_2+\epsilon}$ must have the same topological type as the ambient space $\mathbb{R}^2\times S^1$. But $\mathbb{R}^2\times S^1$ is connected while $V_{\le c_2+\epsilon}$ is disconnected. Hence the equilibrium at q_2 must be a saddle of V.

Next consider the case where $\boldsymbol{w}_{ext}$ induces four equilibria, q_i for $i=1\ldots 4$. Here, too, the assumption $\boldsymbol{w}_{ext}\in\mathcal{W}_{ext}$ implies that one of the equilibria, say q_1, is a local minimum of V. Let $c_i=V(q_i)$ be the critical values of V $(i=1\ldots 4)$, where we may assume that $c_1\le c_2\le c_3\le c_4$. We now show that V must have two local minima and two saddles, by considering three contrarian cases. In case I we assume that V has four local minima. By an argument similar to the one given above, the sub-level set $V|_{\le c_4+\epsilon}$ is topologically equivalent to four disjoint balls—an impossibility since $\mathbb{R}^2\times S^1$ is connected. In case II we assume that V has three local minima and one saddle, say at q_4. Since q_4 has Morse index $\lambda=1$, its Morse data consist of $\mathcal{H}=D^1\times D^2$ which is glued to $\mathcal{G}=S^0\times D^2$ (Table 1). Since $\mathcal{G}$ consists of two disjoint discs, the gluing of $\mathcal{H}$ along $\mathcal{G}$ can connect only two of the three solid balls associated with the local minima. Hence beyond c_4 the sub-level set $V|_{\le c_4+\epsilon}$ remains disconnected—an impossibility since $\mathbb{R}^2\times S^1$ is connected. In case III we assume that V has a single local minimum at q_1 and three saddles. As before, the sub-level set $V|_{\le c_2-\epsilon}$ is topologically equivalent to D^3. At the first saddle a handle $\mathcal{H}=D^1\times D^2$ is glued to D^3 along two disjoint discs. This handle is topologically equivalent to a solid cylinder of finite length (Table 1). Hence $V|_{\le c_2+\epsilon}$, obtained by attaching $\mathcal{H}$ to D^3 along two disjoint discs, is topologically equivalent to a solid torus. The topological change at the remaining two saddles involves the same solid-cylinder gluing operation, giving a two-hole solid torus for $c_3<c<c_4$, and a three-hole solid torus for $c>c_4$. Since V has no critical values beyond c_4, the three-hole solid torus must be topologically equivalent to $\mathbb{R}^2\times S^1$—an impossibility since $\mathbb{R}^2\times S^1$ is topologically equivalent to a single-hole solid torus. We conclude that V must have two local minima and two saddles. □

The following lemma gives the relative value of V at the four equilibria induced by $\boldsymbol{w}_{ext}$, as well as a separation criterion for the basins of attraction of the two local minima.

Lemma 3.5 *Let a planar object $\mathcal{B}$ be grasped by k contacts satisfying the linear contact law (3), such that $\sum_{i=1}^k K_i>0$. Let $\boldsymbol{w}_{ext}\in\mathcal{W}_{ext}$ induce four equilibria, q_i for $i=1\ldots 4$, such*

that q_1 and q_2 are local minima while q_3 and q_4 are saddles of $V(q)$.
Then $V(q_1), V(q_2) < V(q_3) \leq V(q_4)$. In particular, the sub-level set $\{q : V(q) \leq V(q_3)\}$ consists of two topological solid balls touching at q_3 and separated by the fixed-θ planes passing through q_3 and q_4.

Proof: We first establish that $V(d,\theta) = \sum_{i=1}^{k} U_i(q) + U_g(q) + U_{ext}(q)$ is quadratic positive definite in d. The elastic energy induced by the linear contact law (3) is: $U_i(q) = \frac{1}{2}(x_i(q) - y_i^0)^T K_i (x_i(q) - y_i^0) - f_i^0 \cdot x_i(q)$, where $x_i(q) = R(\theta) r_i + d$ for $i = 1 \ldots k$. The gravitational potential energy is given by $U_g(q) = mg\, x_c(q) \cdot \boldsymbol{e}$, where $x_c(q) = R(\theta) r_c + d$. The potential energy corresponding to a fixed force f_{ext} acting at r_{ext} is given by $U_{ext}(q) = -x_{ext}(q) \cdot f_{ext}$, where $x_{ext}(q) = R(\theta) r_{ext} + d$ (a similar expression arises when several forces act at various points of $\mathcal{B}$). Using the notation $\boldsymbol{\rho}_i(\theta) = R(\theta) r_i$, $\boldsymbol{\rho}_c(\theta) = R(\theta) r_c$, and $\boldsymbol{\rho}_{ext}(\theta) = R(\theta) r_{ext}$,

$$\begin{aligned} V(d,\theta) \;&= \tfrac{1}{2} d^T \big(\textstyle\sum_{i=1}^{k} K_i \big) d + d^T \big\{ \sum_{i=1}^{k} K_i \big(\boldsymbol{\rho}_i(\theta) - y_i^0 \big) + mg\boldsymbol{e} - f_{ext} \big\} \\ &\quad + \textstyle\sum_{i=1}^{k} \big\{ \frac{1}{2} \big(\boldsymbol{\rho}_i(\theta) - y_i^0 \big)^T K_i \big(\boldsymbol{\rho}_i(\theta) - y_i^0 \big) - f_i^0 \cdot \boldsymbol{\rho}_i(\theta) \big\} + mg\boldsymbol{\rho}_c(\theta) \cdot \boldsymbol{e} - \boldsymbol{\rho}_{ext}(\theta) \cdot f_{ext}. \end{aligned}$$

Since $\sum_{i=1}^{k} K_i > 0$, $V(d,\theta)$ is quadratic positive definite in d.

Let $c_i = V(q_i)$ be the critical values of V ($i = 1 \ldots 4$), where we may assume that $c_1 \leq c_2$ and $c_3 \leq c_4$. Since $V(d,\theta)$ is quadratic positive definite in d while θ is periodic in 2π, no points are attracted to infinity under the gradient flow $\dot{q} = -\nabla V(q)$. Hence the lowest critical value of V must occur at the local minimum q_1. Suppose now to the contrary, that the next critical value of V occurs at the saddle q_3. According to Morse theory the sub-level set $V|_{\leq c_3 - \epsilon}$ is topologically equivalent to a solid ball D^3. As the value of V passes through c_3, a handle $\mathcal{H} = D^1 \times D^2$ is glued to D^3 along two disjoint discs (Table 1). This handle is topologically equivalent to a solid cylinder of finite length. Hence $V|_{\leq c_3 + \epsilon}$ is topologically equivalent to a solid torus.

We now have two cases to consider. In the first case the next critical value beyond c_3 occurs at the saddle q_4. In this case the sub-level set $V|_{\leq c_4 + \epsilon}$ is topologically equivalent to a two-hole solid torus. When the value of V passes the last critical value c_2, a new *isolated* solid ball appears at the local minimum q_2. The sub-level set $V|_{\leq c_2 + \epsilon}$ therefore consists of two connected components—an impossibility since $\mathbb{R}^2 \times S^1$ is connected. In the second case the next critical value beyond c_3 occurs at the local minimum q_2. Recall now that V is quadratic positive definite in d. Therefore, when a sub-level set of V intersects a fixed-θ plane in $\mathbb{R}^2 \times S^1$, the intersection set must be a single ellipse or a single isolated point. This implies that the solid torus $V|_{\leq c_3 + \epsilon}$ must intersect *every* fixed-θ plane in $\mathbb{R}^2 \times S^1$: otherwise it is confined between two θ planes and must intersect some intermediate θ planes along two disjoint topological discs, contradicting the quadratic positive definiteness of V in d. Beyond c_2, the sub-level set $V|_{\leq c_2 + \epsilon}$ consists of the solid torus and an isolated solid ball which appears at q_2. Since the solid torus intersects every fixed-θ plane in $\mathbb{R}^2 \times S^1$, some θ planes must intersect both sets, contradicting the quadratic positive definiteness of V in d. We conclude that the next critical value of V beyond c_1 must occur at the other local minimum q_2. Thus $V(q_1) \leq V(q_2) < V(q_3) \leq V(q_4)$.

Finally consider the separation criterion between the basins of attraction of q_1 and q_2. Since $V(q_1) \leq V(q_2) < V(q_3)$, the sub-level set $V|_{\leq c_3 - \epsilon}$ consists of two disjoint solid balls, such that all points in the i^{th} ball converge under the gradient flow $\dot{q} = -\nabla V(q)$ to the local minimum at q_i ($i = 1, 2$). The two solid balls meet for the first time at the saddle q_3. The

quadratic positive definiteness of V in d implies that the fixed-θ plane passing through q_3 can intersect these two solid balls only at the isolated point q_3. The two solid balls comprising $V|_{\leq c_3}$ are therefore separated by the fixed-θ plane passing through q_3. Beyond c_3, the sub-level set $V|_{\leq c_3+\epsilon}$ is topologically equivalent to a single solid ball. When the value of V reaches c_4, two locally distinct portions of $V|_{\leq c_4}$ meet at q_4. Here, too, the fixed-θ plane passing through q_4 intersects the sub-level set $V|_{\leq c_4}$ only at the isolated point q_4. Hence the two portions of $V|_{\leq c_4}$ are separated by the fixed-θ plane passing through q_4. Since $V|_{\leq c_3}$ is a subset of $V|_{\leq c_4}$, the fixed-θ plane passing through q_4 also separates the two solid balls comprising $V|_{\leq c_3}$. □

D A Linear Force Displacement Control Scheme

This appendix describes a finger control scheme for achieving a linear force-displacement law at the fingertip. The control law is described for the i^{th} finger and is based on the following assumptions. First, the finger is a fully actuated serial chain having $m \geq 2$ joints, denoted $p_i \in I\!R^m$. The finger ends with a sharp tip whose position is denoted $y_i(p_i)$. Second, the finger is instrumented with ideal joint sensors from which ideal readings of the joints' velocities and accelerations are available. Note that $\dot{p}_i$ and $\ddot{p}_i$ are typically computed from p_i with some measurement noise. Hence our assumption of ideal readings should be revised in future research. Third, we assume knowledge of the finger's geometric and dynamic parameters. Based on these assumptions, we wish to realize a force-displacement law of the form: $f_i = -K_i\big(y_i(p_i) - y_i^0\big) + f_i^0$, where y_i^0 is a fixed setpoint, K_i is a fixed 2×2 positive semi-definite matrix, and f_i^0 is a fixed preload force.

Consider the situation where the fingertip applies a contact force $f_i \in I\!R^2$ on the object $\mathcal{B}$ without contact slippage or breakage. A reaction force $-f_i$ acts on the fingertip and induces joint torques given by $\tau_i = -J(p_i)^T f_i \in I\!R^m$, where $J(p_i) = Dy_i(p_i)$ is the $2 \times m$ Jacobian of $y_i(p_i)$. The finger's dynamics during this interaction is given by

$$M_i(p_i)\ddot{p}_i + C_i(p_i, \dot{p}_i) = u_i - J_i^T(p_i) f_i + \tau_g(p_i), \tag{16}$$

where $M_i(p_i)$ is the finger's $m \times m$ inertia matrix, $C_i(p_i, \dot{p}_i)$ are Coriolis and centrifugal forces, $u_i \in I\!R^m$ is the joints' control input, and $\tau_g(p_i) \in I\!R^m$ are joint torques induced by gravity. The following control law consists of two parts. The first part compensates for the finger's inertial forces as well as gravity. The second part imposes joint torques according to the linear force-displacement law:

$$u_i(p_i, \dot{p}_i, \ddot{p}_i) = M_i(p_i)\ddot{p}_i + C_i(p_i, \dot{p}_i) - \tau_g(p_i) + J_i^T(p_i)\big(-K_i(y_i(p_i) - y_i^0) + f_i^0\big). \tag{17}$$

Substituting for u_i in (16) gives the closed loop finger dynamics:

$$J_i^T(p_i)\big\{\big(-K_i(y_i(p_i) - y_i^0) + f_i^0\big) - f_i\big\} = \vec{0}. \tag{18}$$

The argument of $J_i^T(p_i)$ in (18) vanishes in the generic case where $J_i^T(p_i)$ has full rank. Therefore, as long as the fingertip maintains a non-sliding contact with $\mathcal{B}$, the finger's closed-loop dynamics dictates that f_i satisfies the desired linear force-displacement law: $f_i = -K_i\big(y_i(p_i) - y_i^0\big) + f_i^0$. An experimental investigation of this control approach is under progress and will be reported in a future paper.

References

[1] A. Bicchi. On the problem of decomposing grasp and manipulation forces in multiple whole-limb manipulation. *Int. J. of Robotics and Autonomous Systems*, 13(4):127–147, 1994.

[2] A. Bicchi. Hands for dexterous manipulation and robust grasping: A difficult road toward simplicity. *IEEE Trans. on Robotics and Automation*, 16(6):652–662, 2000.

[3] N. Brook, M. Shoham, and J. Dayan. Controllability of grasps and manipulations in multi-fingered hands. *IEEE Trans. on Robotics and Automation*, 14(1):185–192, 1998.

[4] R. C. Brost and R. R. Peters. Automatic design of 3-D fixtures and assembly pallets. *Int. J. of Robotics Research*, 17(12):1243–1281, 1998.

[5] M. R. Cutkosky and I. Kao. Computing and controlling the compliance of a robotic hand. *IEEE Trans. on Robotics and Automation*, 5(2):151–165, 1989.

[6] M. R. Cutkosky and P. K. Wright. Friction, stability and the design of robotic hands. *Int. J. of Robotics Research*, 5(4):20–37, 1986.

[7] M. A. Erdmann. On motion planning with uncertainty. Technical Report AI-TR-810 (MS Thesis), MIT AI Lab, Aug 1984.

[8] M. A. Erdmann. On a representation of friction in configuration space. *The Int. J. of Robotics Research*, 13(3):240–271, 1994.

[9] Goresky and Macpherson. *Stratified Morse Theory*. Springer-Verlag, New York, 1980.

[10] H. Hanafusa and H. Asada. Stable prehension by a robot hand with elastic fingers. In Brady et al., editor, *Robot Motion*, pages 322–335. MIT Press, 1982.

[11] K. Harada and M. Kaneko. A sufficient condition for manipulation of enveloping family. *IEEE Trans. on Robotics and Automation*, 18(4):597–607, 2002.

[12] S. Huang and J. M. Schimmels. The bounds and realization of spatial stiffnesses achieved with simple springs connected in parallel. *IEEE Trans. on Robotics and Automation*, 14(3):466–475, 1998.

[13] S. Huang and J. M. Schimmels. The bounds and realization of spatial stiffnesses compliances achieved with simple serial elastic mechanisms. *IEEE Trans. on Robotics and Automation*, 16(1):99–103, 2000.

[14] K. L. Johnson. *Contact Mechanics*. Cambridge University Press, 1985.

[15] D. E. Koditschek. The application of total energy as a lyapunov function for mechanical control systems. *In J. Marsden, P. Krishnaprasad, and J. Simo, editors, Control Theory and Multibody Systems, AMS Series in Contemporary Mathematics*, 97:131–158, 1989.

[16] G. F. Liu, J. Li, and Z. X. Li. Coordinated manipulation of objects by multifingered robotic hand in contact space and active joint space. In *IEEE Int. Conf. on Robotics and Automation*, pages 3743–3748, 2002.

[17] J. W. Milnor. *Morse Theory*. Princeton University Press, Princeton, NJ, 1963.

[18] J. W. Milnor. *Topology from the Differentiable Viewpoint*. The University Press of Virginia, 1965.

[19] D. J. Montana. Contact stability for two-fingered grasps. *IEEE Trans. on Robotics and Automation*, 8(4):421–230, 1992.

[20] V.-D. Nguyen. Constructing force-closure grasps. *The Int. J. of Robotics Research*, 7(3):3–16, 1988.

[21] T. Omata and K. Nagata. Rigid body analysis of the indeterminate grasp force in power grasps. *IEEE Trans. on Robotics and Automation*, 16(1):46–54, 2000.

[22] C. Ott and Y. Nakamura. Resolving the non-integrability of nullspace velocities for compliance control of redundant manipulators by semi-definite Lyapunov functions. In *IEEE Int. Conf. on Robotics and Automation*, pages 1999–2004, 2008.

[23] J. Ponce. On planning immobilizing fixtures for 3D polyhedral parts. In *IEEE Int. Conf. on Robotics and Automation*, pages 509–514, 1996.

[24] J. Ponce, S. Sullivan, A. Sudsang, J.-D. Boissonnat, and J.-P. Merlet. On computing four-finger equilibrium and force-closure grasps of polyhedral objects. *The Int. J. of Robotics Research*, 16(1):11–35, February 1997.

[25] F. Reuleaux. *The Kinematics of Machinery*. Macmillan 1876, republished by Dover, NY, 1963.

[26] E. Rimon, S. Shoval, and A. Shapiro. Design of a spider robot for motion with quasistatic force constraints. *Autonomous Robots*, 10:279–296, 2001.

[27] K. Y. Rong, S. H. Huang, and Z. Ho. *Advanced Computer-Aided Fixture Design*. Elsevier, Boston, 2005.

[28] J. K. Salisbury. *Kinematic and Force Analysis of Articulated Hands*. PhD thesis, Dept. of ME, Stanford University, 1982.

[29] T. Schlegl, M. Buss, T. Omata, and G. Schmidt. Fast dextrous regrasping with optimal contact forces and contact sensor-based impedance control. In *IEEE Int. Conf. on Robotics and Automation*, pages 103–108, 2001.

[30] A. Shapiro. *Design and Control of an Autonomous Spider-Like Robot*. PhD thesis, Dept. of Mechanical Engineering, Technion, 2003, http://robots.technion.ac.il.

[31] A. Shapiro, E. Rimon, and J. W. Burdick. Passive force closure and its computation in compliant-rigid grasps. In *IEEE/RSJ Int. Conference on Intelligent Robots and Systems* (IROS), 2001.

[32] A. Shapiro, E. Rimon, and S. Shoval. On the passive force closure set of planar grasps and fixtures. Tech. report, Dept. of Mechanical Engineering, Technion, http://robots.technion.ac.il/publications, Dec. 2008.

[33] K. B. Shimoga and A. A. Goldenberg. Constructing multifingered grasps to achieve admittance center. In *IEEE Int. Conf. on Robotics and Automation*, pages 2296–2301, 1992.

[34] J. C. Trappey and C. R. Liu. A literature survey of fixture design automation. *The Int. J. of Advanced Manufacturing Technology*, 5(3):240–255, 1990.

[35] C. Xiong, H. Ding, and Y. Xiong. *Fundamentals of Robotic Grasping And Fixturing*. Series on Manufacturing Systems and Technology, World Scientific, 2007.

[36] C. H. Xiong, Y. F. Li, H. Ding, and Y.-L. Xiong. On the dynamic stability of grasping. *The Int. J. of Robotics Research*, 18(9):951–958, 1999.

[37] C.-H. Xiong, M. Y. Wang, Y. Tang, and Y.-L. Xiong. Compliant grasping with passive forces. *J. of Robotics Systems*, 22(5):271–285, 2005.

[38] T. Yoshikawa. Passive and active closure by constraining mechanisms. *J. of Dynamic Systems, Measurement, and Control*, 121 (3-4):418–424, 1999.